A Thesis

entitled

An analysis of NO_x and PM emissions in idling and moving conditions of buses with EGR and Non-EGR engines running on biodiesel

by

Manideep Yarlagadda

Submitted to the Graduate Faculty as partial fulfillment of the requirements for the Master of Science Degree in Civil Engineering

Dr. Ashok Kumar, Committee Chair

Dr. Dong-Shik Kim, Committee Co-Chair

Dr. Liangbo Hu, Committee Member

Dr. Amanda Bryant-Friedrich, Dean
College of Graduate Studies

The University of Toledo
December 2016

An Abstract of

An analysis of NO_x and PM emissions in idling and moving conditions of buses with EGR and Non-EGR engines running on biodiesel

by

Manideep Yarlagadda

Submitted to the Graduate Faculty as partial fulfillment of the requirements for the Master of Science Degree in Civil Engineering

The University of Toledo
December 2016

Biodiesel is an alternate to diesel for transit buses due to its environmental benefits. However, NO_x and particulate matter emissions may be an issue in the use of biodiesel. The major objective of this experimental thesis was to study tail pipe emissions from transit buses during daily routine operations. This thesis focuses on the trends of NO_x and particulate matter emissions collected from buses with EGR and NON-EGR engines during their total run times. To further categorize and elaborate our findings, the run time was divided into both idling and running conditions.

In order to achieve comprehensive results, the idling and running conditions were further segregated into two different cases, i.e., cold idling and hot idling conditions. The running conditions were divided into acceleration, deceleration, motion in variable speeds and partial idle modes. The NO_x emission values were collected and analyzed for all the conditions and modes described above. The particulate matter emissions were collected and analyzed in idle conditions. It was learned that hotter engines produced lower emissions when compared to cold engine conditions. The experiments and analysis of NO_x emissions concluded that maximum emissions were found in the acceleration condition.

A Mexa-720 Horiba NO_x analyzer was used to measure NO_x emissions and Cummins in-site 6 equipment and software program were used for engine data collection

during the field study. The experiments were carried out on both transit buses with EGR and NON-EGR engines. The particulate matter emissions collection was carried out with quartz filter papers and a CATCH CAN instrument. An EDS X-Max 50mm2 / FEI Quanta 3D FEG Dual Beam Electron Microscope was used for the EDS analysis of PM emissions and the ICP-MS was carried out using Xseries 2. The transit buses are used by Toledo Area Regional Transit Authority (TARTA). Both the buses were fueled with B5 grade biodiesel without making any engine modifications and the study was conducted during the summer and fall of 2015.

The emission values were collected along with the consideration of various engine parameters such as engine temperature, exhaust gas pressure, fuel flow rate command, diesel oxidation catalyst intake temperature and the diesel particulate filter intake temperature. The collected NO_x emission values were analyzed, as a function of time, with the help of three different regression techniques and obtained the best results with the Random Forest Regression algorithm. A NO_x emission prediction model was established as a function of the engine parameters using the field data and regression results. Elemental analysis was performed on the particulate matter emissions and it was concluded that trace metal and carbon concentrations were higher in the NON-EGR engine buses in comparison to the EGR engine buses.

I dedicate this work to my family

Acknowledgments

First and foremost, I would like to express my deep gratitude to my advisor and thesis committee chairman, Dr. Ashok Kumar for all of the kind and enthusiastic motivation, support and guidance that he has provided me with over the course of my masters.

I would like to offer my special thanks to my co-advisor, Dr. Dong-Shik Kim for his valuable and constructive suggestions during the period of my research work. His willingness to give his time so generously has been very much appreciated.

I thank Dr. Liangbo Hu for being in my committee and for his benevolent and gracious guidance.

I would also like to thank the Civil Engineering Department and USDOT/MNTRC for the financial assistance and TARTA for authorizing me to use their buses for my research.

I thank Ruthwik Junuthula and Nader for helping me with my thesis analysis, and Sai Kameshwar Nittala, Jahnavi Yalamanchili, Venkatesh Chalasani, Harsha Rahul thati, Ashok Tummala for helping me with documentation. I appreciate the help provided by Sudheer Kumar Kuppili and Mounika Sajja.

Most importantly, I would like to thank my family for their continuous love and support.

Contents

List of Tables

List of Figures

Chapter 1

Introduction

In our daily lives, engaging in various physical and mental activities such as recreation, travel and spending time at home often leads to a large number of health risks. These risks can be evaded by making the right decisions and being diligent to avoid health problems. Numerous studies have pointed out a direct correlation between the exposure to pollutants emitted from diesel exhaust and the increasing rates of mortality, respiratory and cardiovascular problems [1].

A survey conducted by the Texas Transportation Institute revealed that Americans on an average spent about 6.9 billion hours commuting in the year of 2014 as compared to the 6.4 billion hours in the year 2010 spent commuting. This was mostly to travel between their place of residence and work, of which a large percentage was spent in traffic [2]. A recent study on population explosion in the country revealed that that the person to car ratio was found to be at astonishing rate of 1:1.3 [3].

Over the last couple of years, many Americans have switched their transportation methods from personal vehicles to public transit in order to cut down on time spent in commuting. In 2014, the American Public Transportation Association(APTA) [4] released a report stating that 10.8 billion trips were made on public transportation in that particular year alone which stood out to be the highest annual public transit ridership number over the last few decades [5].

A few noteworthy facts derived from the Public Transportation Fact Book published in 2013 and other research papers are:

1. Transit buses accounted to more than 5000 million miles in passenger trips in the year 2011 which was estimated to be 51.3% of the total transit miles covered in passenger trips followed by heavy rails which ran for about 3647 million miles.

2. In the year 2011, transit vehicles were operated for 313 million hours of revenue service of which transit buses were operated for 161.1 million hours.

3. The average cost of a transit bus lies anywhere between $400,000 and $600,000 and has a useful life of about 12 years after which it is withdrawn from the roads [6].

4. An estimated 2117 million gallons of diesel was consumed by transit buses, representing nearly 7% of the total diesel consumption in the United States of America.

5. A transit bus travels around 150,000 miles annually, utilizing close to 50,000 gallons of fuel with a mileage of 3 miles per every gallon.

Automobiles travelling on highways move at constant speeds which imply that the engine runs smoothly without abrupt changes in acceleration and braking modes. The same is not the case with vehicles travelling in city limits due to the traffic and speed limits imposed. Transit buses also have to deal with periodically occurring passenger bus stops where they come to rest for a brief period ranging from a few seconds to minutes. In addition to this, the time spent at the signals and stop signboards also account for an increase in idle time. These transit buses are said to be operated on a stop-and-go driving style which involves instant acceleration and constant braking thereby leading to heavy emissions of air pollutants and reduction in the mileage of the vehicle.

Individuals are highly vulnerable to the effects of these emissions and action can only be taken by public authorities acting on a national and global level. In a report by the World Health Organization in 2006, it was estimated that more than 2 million premature deaths each year can be attributed to these air pollutants [7].

Fuel combustion in vehicles produces pollutants such as carbon moNO_xide (CO), carbon dioxide (CO_2), hydrocarbons (THC), volatile organic compounds, Nitrogen Oxides (NO_x) and Particulate Matter (PM).

Carbon MoNO_xide is produced from the incomplete combustion of fuel and is emitted directly from the exhausts of motor vehicles [8, 9]. The carbon moNO_xide so formed reacts with other pollutants in the air to produce ozone which is harmful at the ground level. High concentrations and long term exposure may result in serious health problems (Scottish Environment Protection Agency).

Carbon dioxide accounted for about 82% of all U.S. greenhouse gas emissions in 2013, a 5 percent rise over a period of 8 years [10]. Carbon dioxide is formed due to both natural and human sources. Ever since the industrial revolution, concentrations of carbon dioxide have increased to dangerous levels which affect human health and the environment resulting in global warming.

Hydrocarbon emissions in major concentrations are produced when the engine fuel does not burn or burns partially, which leads to formation of ozone which is one of the vital components in the production of smog. Ozone and smog cause serious health issues such as damage to the lungs and also causes serious respiratory diseases. Most hydrocarbons are toxic and may lead to cancer. Total hydrocarbon (THC) emissions are the most widespread air pollutants [11].

Volatile organic compounds are dangerous to both the environment and human health as exposure to air can result in acid rain, flame production and cause serious damage to eyes and lungs. The compounds in their dormant stage are not too harmful but they do interact with other gases and compounds to contribute to air pollution.

Nitrogen oxides are known to be highly reactive gases. These are caused as a result of burning of fuel at high temperatures and are the most crucial components in the air polluting chemical compounds. They have huge effects on global warming alongside the carbon compounds. The primary form of these nitrogen oxides are in the form on nitric oxide (NO) which reacts with oxygen in the atmosphere to produce nitrogen dioxide leading to acid rain. Automobiles are credited for more than half of all nitrogen oxide emissions in the United States of America [12].

A mixture of the solid particles and liquid droplets found in the air constitute particulate matter (PM). Smoke, dirt and soot are some of the particles which come under PM and come in various shapes, sizes and compositions. Fuel combustion produces a large quantity of PM of 10 micrometers in diameter or smaller and is regulated by EPA according to their sizes [1]. PM of fine sizes is a major concern for human health as it can reach the deepest places in the organs. Diesel exhaust particle emissions are considered to be a carcinogen and are therefore defined as toxic [1, 13]. Reports have proved that PM from automobiles have had more serious health impacts than that produced from other sources [14].

All the emissions compounds discussed above are the end results of the combustion of fuels and pose a serious threat to mankind. Over the years, EPA has set emission standards for the major contributors to air pollution in order to control the amount and types of harmful emissions released into the environment and are tabulated in Table 4.9.

As observed from Table 4.9, there have been considerable changes to the standard levels of nitrogen oxide compounds NO_x and particulate matter (PM) over the years stating the importance of controlling the emissions of these type of compounds due to their high adverse effects.

A detailed literature review conducted on emissions obtained from transit buses proved that very few studies have been performed on tail pipe emissions for buses

Table 1.1: EPA emissions standards (g/km)

Emmission standards	**CO**	**THC**	**NO$_x$**	**NHMC**
1994	45.06	3.78	14.54	
1996	45.06	3.78	11.63	
1998	45.06	3.78	11.63	
2004(1)	45.06	3.78		
2004(2)	45.06	3.78		2.91
2007	45.06	3.78	3.92	0.41
2010	45.06	3.78	0.58	0.41
2016			0.96	0.15

(Source: Transit Cooperative Research Program, 2016)

running on bio-diesel. Although the studies focused on tail pipe emissions, there was not much discussion on tail pipe emissions in running condition of buses.

The major drawbacks in most of these studies, given in section 2.4, have been the small size of vehicle fleet and also the need to collect engine and emission data simultaneously to study the effect of engine parameters on emissions [15–18]. To obtain a more comprehensive view and to fill the knowledge gap between exhaust emissions from transit buses, a detailed study was conducted and the framework of the study is as follows:

1. Obtaining emission values from buses in running conditions considering all operating parameters (passenger loads, traffic, and climate).

2. The data collection in running conditions was split into four different scenarios based on speed namely- initial acceleration, moving with variable speed, deceleration condition and idle positions.

3. Idling position values were obtained from both cold and hot idling conditions with more than five engine parameters being considered. For all the above

conditions, data were collected from the buses equipped with exhaust gas recirculation (EGR) and non-exhaust gas recirculation (Non-EGR) engines.

4. Simultaneously, particulate matter (PM) samples were collected from tail pipe emissions of both EGR and Non-EGR equipped buses and a detailed elemental analysis and compound concentrations were determined.

This research employed three different regression to analyze the obtained NO_x emission values as a function of time and RPM from running conditions and to determine the method with the least error among the tested methods. These methods were compared and the most accurate method for determining NO_x emission values was established which can be used for future work and as references. The regression techniques were also employed to analyze multivariate engine data from transit buses in idle conditions and to identify the true influence of the different variables. The impacts of the engine parameters on NO_x emission values were investigated in order to determine which engine parameter has the largest influence on the NO_x emission values.

To achieve the objectives, one fleet of buses with exhaust gas recirculation (EGR) equipped engine and another fleet of buses with non-exhaust gas recirculation (Non-EGR) equipped engine from the Toledo Area Regional Transit Authority (TARTA) buses were chosen.

In Toledo, Ohio, TARTA has been the "Ride of Toledo" since 1971 and has over 40 routes in the metropolitan area, serving nine communities and carrying almost 5 million passengers annually. These buses cater to Northwest Ohio's entire public transportation needs. With over 230 buses operating throughout a day, TARTA buses contribute to a significant percentage of total emissions in the region. To contribute its share for the importance of a cleaner environment, TARTA started adopting the use of alternative diesels including B20 and ULSD fuels since June 2006. Over the past couple of years, TARTA replaced B20 grade biodiesel with B5 grade biodiesel. To study NO_x emissions and PM emission values, a 701 bus equipped with a Non-EGR engine and an 802 bus equipped with an EGR engine from 700 and 800 series, respectively [19].

Experiments were carried out on B5 fueled compression ignition engines. A Horiba NO_x analyzer was employed to calculate NO_x emission values from the exhaust pipe. A Cummins in-site 6 bridge was used to calculate engine data from the transit bus. For the 800 series bus, a 9 pin plug connector is used for the engine data collection, whereas for the 700 series bus, a 6 pin plug connector is used. Particulate matter emissions were collected on quartz filter papers.

The research aims to use the above collected information to study the impacts of using alternative diesel technology (biodiesel) on NO_x & PM concentrations and to determine the NO_x emission values by developing predictive models and equations for TARTA buses.

The following thesis is organized into 4 chapters. Chapter 2 gives a literature review of vehicular emissions. Chapter 3 discusses in detail the methodology followed for data collection and the experimental design carried out for analyzing the data gathered. Chapter 4 includes the results and provides a statistical review of the results obtained from the data analysis. The conclusion of the thesis includes the key findings and recommended future works which are discussed in Chapter 5.

Chapter 2

Literature Review

2.1 Health Effects

Diesel engines require less maintenance and generate more pollution. Over 40 chemicals from diesel exhausts are considered as toxic air contaminants. The exhaust emission composition primarily depends upon the composition of fuel, temperature at which it burns, engine, tire and operating conditions. [20] demonstrated an association between different levels of air pollution and health outcomes involving mortality, chronic bronchitis,and respiratory tract infections. These emissions also have profound impacts on the environment, production of smog, acid rains, hydrocarbons and air toxins. These can affect plants, animals, and water resources [21]. Epidemiological studies shows that the risk of lung cancer among people having been exposed to diesel exhaust is approximately 1.2 to 1.5 times more than the people who are not exposed. Table 2.1 summarizes the environmental and health effects caused by the exhaust emissions from diesel engines.

After the emission from tailpipes, these pollutants undergo atmospheric transformations that may change the toxic properties of the original pollutants, creating by-products that may be more hazardous. EPA estimates that every 1 dollar spent on clean diesel projects produces up to 13 dollars of public health benefits [12].

Table 2.1: Environmental and health effects caused due to diesel exhaust

Acute Effects	Chronic Effects	Environmental Effects	Possible Improvements
Irritation of eyes,nose, and throat	Lung cancer	Ozone formation	Use of Cleaner burning and renewable fuels (natural gas, propane,electricity)
Cough, headache, dizziness	Bronchitis	Acid rain	Retro-fitting of nausea, and reduce lung function existing engines with in children particle filters
Heartburn, chest tightness, wheezing, vomiting, and increase the frequency of asthma attacks	Respiratory and heart diseases	Global climate Change	Use of new diesel engines of advanced technologies that produce 90% lesser particle emissions
Damage of respiratory and central nervous system	Pneumonia	Visibility issues and haze	
When exposed to higher levels: coma, convulsions, and death	Emphysema, & Premature deaths		

(Source: Compiled from U.S. EPA, Factsheet: USACHPPM)

2.2 National Ambient Air Quality Standards

The U.S. Environmental Protection Agency (USEPA) is required to set National Ambient Air Quality Standards (NAAQS) to protect environment from air pollutants as per the Clean Air Act, amended in 1963. The Clean Air Act has identified two types of air quality standards namely primary and secondary standards. Standards required to maintain public health protection are known as primary standards and standards required for maintaining and providing public welfare protection are known as secondary standards.

The USEPA has set NAAQS for six principal pollutants, known as criteria air pollutants which are periodically reviewed and revised. Table 2.2 gives a detailed description of the present levels for these criteria air pollutants. The units of measure are parts per million (ppm) by volume, parts per billion (ppb) by volume, and micrograms per cubic meter of air (μg/m3).

Table 2.2: NAAQS Table (μg/m^3)

Standard Type	**Pollutant**	**Averaging Time**	**Standard Level()**
Primary	Carbon moNO$_x$ide	8-hour	9ppm
Primary	Carbon moNO$_x$ide	1-hour	35ppm
Primary & Secondary	Nitrogen Dioxide	Annual	53ppb
Primary & Secondary	Ozone (O_3)	8-hour	0.070 ppm
Primary	Particulate Matter ($PM_{2.5}$)	1 year	12.0 μ g/m^3
Primary & Secondary	Particulate Matter ($PM_{2.5}$)	24-hour	35 μ g/m^3
Primary & Secondary	Lead	3-month	0.15 μ g/m^3
Primary	Sulphur Dioxide (SO_2)	1-hour	75 ppb
Secondary	Sulphur Dioxide (SO_2)	3-hour	0.5 ppm

(Source: USEPA (https://www.epa.gov/criteria-air-pollutants/naaqs-table), accessed-March-2016

2.3 Fuel Standards

With increased emissions over the years, there has been a growing concern among countries for the safety and health of humans and environment. Emissions from vehicles mainly depends on the type of fuel used. With fossil fuel reserves on the verge of depletion and stricter emission standards, various fuel alternatives are being considered. Compressed Natural Gas (CNG), diesel and biodiesel are some of the fuels which are widely used in vehicles. The USEPA mandated the use of Ultra-Low Sulfur Diesels (ULSD) starting in 2006. The sulfur content in ULSD ranges from 15-30ppm while that in regular diesel has a maximum of 500 ppm. [22] enables the use of emission reduction equipment like particulate traps.

Biodiesel is another alternative fuel which is being used in an increasing number of automobiles. It is made from a blend of animal fats and vegetable oils and is generally operated in compression-ignition engines. It greatly reduces emissions of hydrocarbons, carbon moNO_xide and particulate matter but there is a noted increase in NO_x emissions and is less energy-efficient [23].

2.4 Previous Studies on Vehicular Emissions

Conventional diesel is a mixture of hydrocarbons extracted from petroleum. It costs less than gasoline as the extraction process is cheaper. The test procedures defined by the USEPA in the Code of Federal Regulations in the United States state that diesel engines are regulated for CO, NO_x, THC and PM emissions. In order to reduce these emissions and the usage of non-biodegradable fuels, efforts are being carried out to develop alternative diesel fuels and blends throughout the world.

Some of the alternative fuels include biodiesel, compressed natural gas, liquefied petroleum gas, alcohol fuels (methanol, ethanol) and hydrogen. Each of the above mentioned fuels has reductions in emissions of one or more primary pollutants and can be assessed to determine the suitability for different applications. Biodiesel can be obtained from sunflowers, soybeans, animal fats or used cooking oil. This reduces PM, CO, THC emissions, but produces increased NO_x emissions. Compressed natural gas can be collected from underground reserves and reduces all primary pollutant emissions except hydrocarbons. The major disadvantage in the use of CNG is that it is not easily accessible and procured. CNG vehicles cost around $7,000 - $12,000 more than gasoline or diesel cars. Ethanol can be derived from starch crops, corn, wheat and agricultural waste. It helps reduce ozone forming emissions by 25% when compared to petro-diesel. The major drawback of using ethanol as a fuel is its highly corrosive nature which will eventually lead to lower operating life of the engines. Hydrogen is also being used as an alternate fuel and can be procured from natural gas and electrolysis but has no major reduction in emissions when compared to gasoline. Liquefied petroleum gas is also used as a major alternate fuel and is formed as a by-product of petroleum refining. It reduces CO_2 emissions but there is an increase in NO_x emissions.

From the above discussion, it can be inferred that biodiesel, having similar properties to that of conventional diesel is gaining popularity as an alternate fuel because it can be derived from renewable sources. Biodiesel is basically made up of mono-alkyl esters of medium to long chain of fatty acids formed by the process of trans-esterification of organic oils [6]. It is biodegradable and non-toxic and most importantly, it can be substituted with conventional diesel with almost no engine modifications. It also possesses the characteristic that cleans carbon depositions inside a combustion chamber. Due to its above mentioned properties, a legislation was passed by the congress as a part of the Energy Conservation Reauthorization Act of 1998, which allows federal and state fleet to use 20% or higher biodiesel blends. It can also be easily transported. The USEPA had conducted an analysis on the emission impacts of using biodiesel. The study used data which was collected on heavy

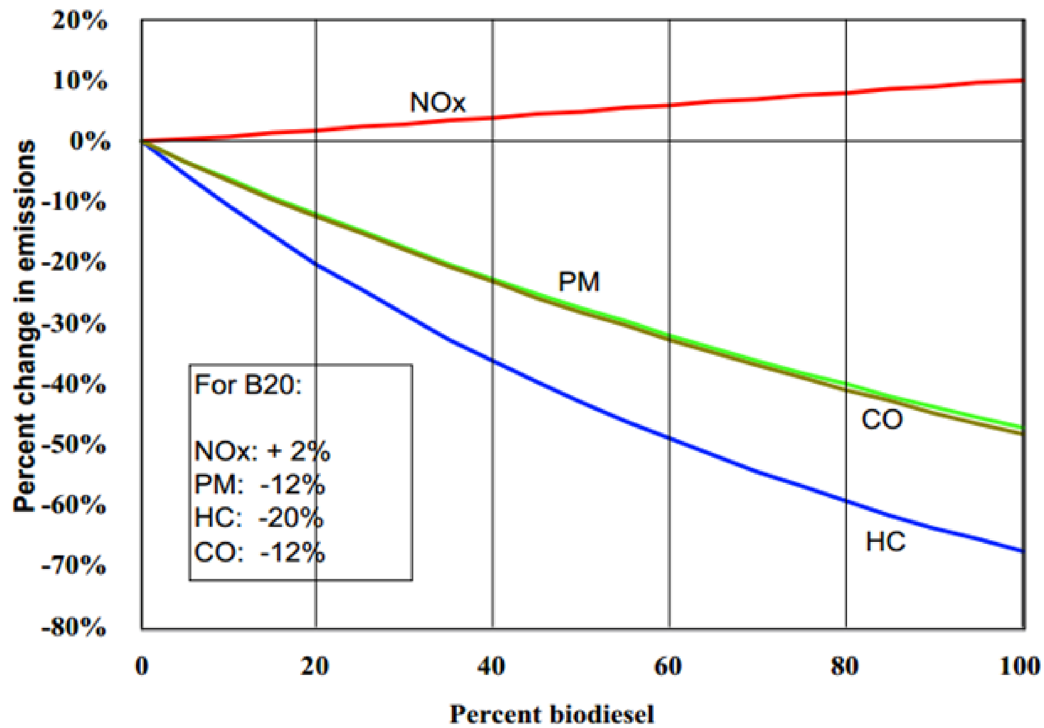

Figure 2-1: Change in emissions due to change in % biodiesel

(Source: USEPA)

duty-highway engines and statistical regression analysis was used to investigate the data collected. The average effects of each pollutants are shown in Fig. 2-1.

According to a study conducted by [24], emission values depend mainly on driving behavior (speed, acceleration or speed time acceleration), road conditions and on driving habits. The most important parameters which affect the emission rates of pollutants are presented in the Fig. 2-2 [25].

Although there is an agreement on the overall reduction of emissions in utilizing biodiesel, the percentage reduction varies from study to study due to the different oil feed stocks used as sources. A comprehensive analysis of the emission impacts of biodiesel on heavy duty highway engines was conducted by the US EPA which showed that the estimated impacts for any soy bean based B20 biodiesel noted a decrease of

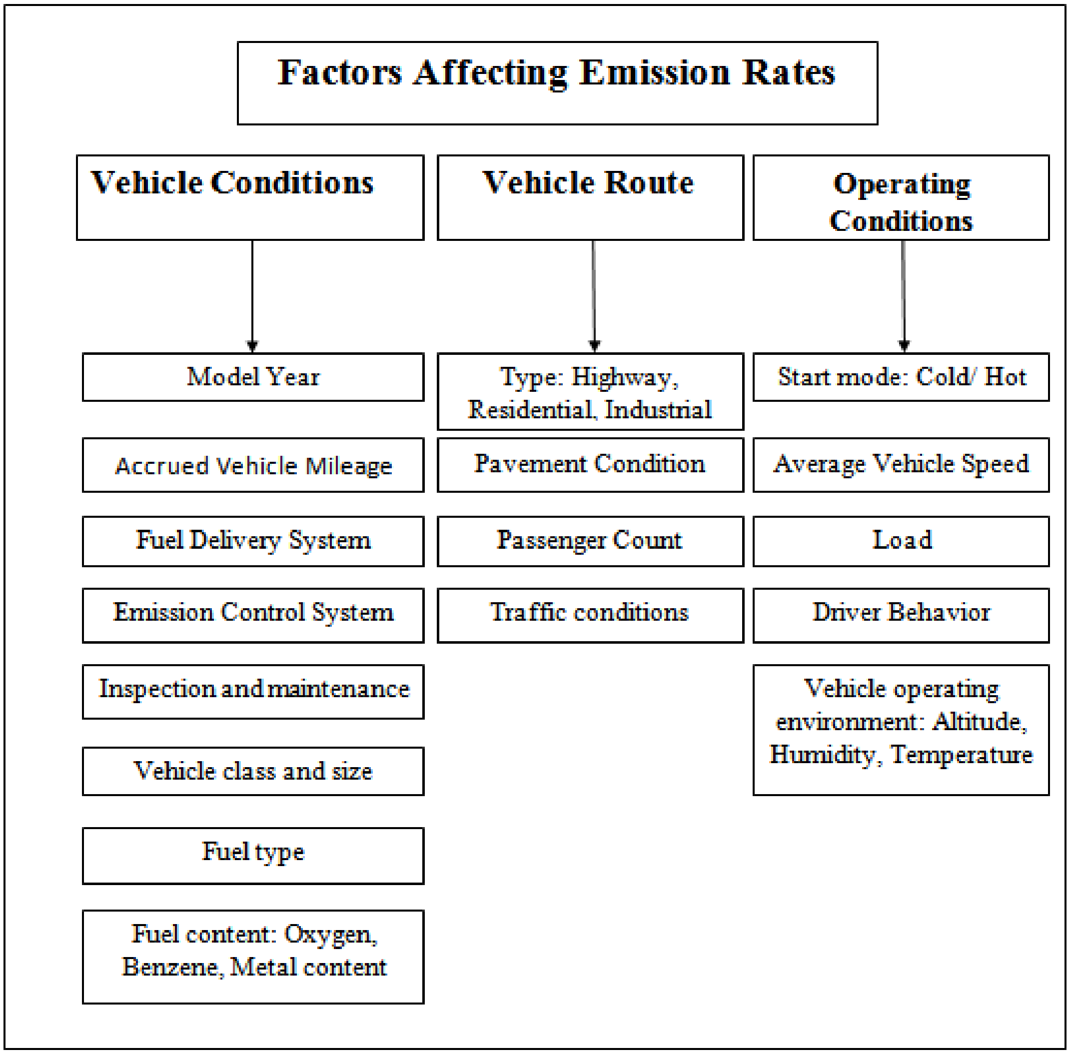

Figure 2-2: Factors affecting emission rates

21.2% of hydrocarbon, 11% decrease in CO, 10% decrease for PM and a 2% increase for NO_x emissions. In 2005, a study conducted by [26] used bio-diesel blends derived from soy bean and found a 6-9% increase in NO_x emissions when compared to petro-diesel [27, 28]. In 2005 observed that there was a 25% decrease in particulate matter and NO_x emissions had increased by about 3% in all engines using biodiesel. [29] used a non-edible Jatropha oil-based biodiesel to compare performance, emission and combustion characteristics of biodiesel and diesel fuel. They concluded that HC, CO and CO2 emissions were lower with Jathropa biodiesel but there was an increase in

NO_x emissions. [30] used sunflower and cottonseed oil methyl esters of Greek origin as supplements in the diesel fuel as B10 grade (10/90) and B20 grade (20/80) and concluded that both these blends had reduced emission potential of pollutants like carbon moNO_xide and hydrocarbons in contrast to the engines fueled with ultra-low sulfur diesel (ULSD).

The three distinct sources of air pollution from motor vehicles are combustion process, wear of tires and brakes,and evaporation of fuel. Emissions from combustion process depend on the ambient temperature, power output of engine, fuel characteristics and emissions control systems [14, 31]. Evaporation of fuel is mainly the hydrocarbon vapors let in to the atmosphere from the carburetors and fuel tank. Carburetor loss is known as hot soak emissions and mainly occur when a hot engine is stopped. Fuel tank loss is mainly due to the diurnal and temperature changes

Emissions not only depend on various types of fuels but also depend on different engine parameters (engine temperatures, speeds, etc.). In the year 2005, [32] presented that the cold start emission rates were higher than the extended idling emission rates where he determined cold start time as ten minutes after the engine was started and the extended idling period constituted the time when the emissions reached its steady state. He proved his hypothesis by showing that the cold start emission rates were higher by factors of 2.5 for CO, 1.5 for NO_x and 1.7 for $PM_{2.5}$. The average emissions from the extended idling condition for CO, NO_x and $PM_{2.5}$ were 64.5 167 and 3.51 g/hr., respectively. [33] had performed PM emission analysis to show that mean value of emission of PM was not only depended on the fuel type but also on the engine conditions.

[34] presented a theory to explain the increase in NO_x emissions while using biodiesel was due to the chemical structure of biodiesel as it had more double bonds than conventional diesel. [15] concluded that a significant factor affecting NO_x emissions is the combustion temperature whereas for PM it depends on fuel composition

and molecular structure. [35] pointed out that the increased NO_x emissions while using biodiesel can be mitigated by modifying the engine control settings mainly by increasing the exhaust gas recirculation. Exhaust Gas Recirculation (EGR) refers to a NO_x emission reduction technique employed in diesel/gasoline engines, where a portion of the exhaust gas is recirculated back to the engine cylinders. They concluded that the absolute value of NO_x emissions from biodiesel combustion appeared to be reduced when EGR equipped engines were used where the percentage change was substantial. He also pointed out that a long term study was required as this has been used for commercial use for a short time.

[33] developed emissions models that explain the relationship for exhaust emission pollutants by identifying the factors affecting the actual emissions from transit buses. According to their model, fuel rate, engine load, engine and exhaust temperatures and engine rpm are the most important variables which affect the concentration of pollutants. From their findings, they concluded that by reducing the idle time during long durations of idling vehicular impact on air quality can be reduced by large extents.

While conducting field experiments on the on board systems representing actual running conditions, [16, 36] concluded that the average emissions from biodiesel in the acceleration mode were 5 times greater than the idle modes for hydrocarbons and carbon dioxide and 10 times greater for nitric oxide and carbon moNO_xide when working with gasoline and a blend of 85%ethanol and 15% gasoline (E85). In addition, [27, 37] conducted chassis dynamometer studies on heavy vehicles with B10 grade biodiesel and indicated that there was a significant decline in PM, CO and THC emissions over the years but there was no notable change in NO_x emissions. They have also conducted remote sensing studies pointing out that NO_x emissions were normally distributed for most high emitting diesel vehicles. Both [27, 36] faced numerous difficulties while collecting the data due to the fact that environmental

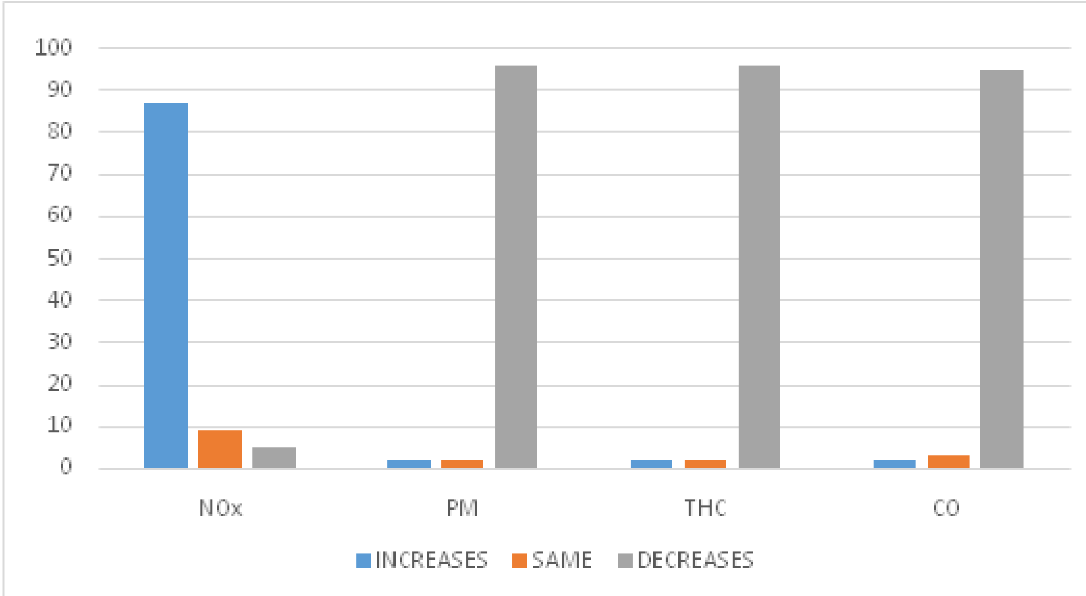

Figure 2-3: Estimated share of literature (in percentage of number of publications) on Emissions using biodiesel and diesel fuels

factors affect the data collection procedure.

[32, 38] published a detailed review on exhaust emissions from biodiesel powered heavy vehicles. A summary of the majority of studies conducted by previous researchers including the emission results, reported increases, similarities and decreases, in various categories of pollutants. An increase in emissions of NO_x, CO and THC are noted as seen in Fig. 2-3.

The major drawback of using biodiesel fuels is not only the increase in NO_x emissions, but biodiesel also causes clogging in engine filters, has a short shelf-life and is not suitable for operation in low temperature regions. Biodiesel fuels are also about one and a half times more expensive than conventional diesel fuels [15]. Again, however, biodiesel offers advantages such as less engine wear, extended life of catalytic converters, easy distribution through existing diesel pumps (Berkeley biodiesel). [6] showed that ULSD fuel had low lubricity when compared to biodiesel. [39] conducted a study to show that lubricants were required to be added to biodiesel to enhance the lubricity in order to reduce the engine wear. This was attributed to the fact that biodiesel contains no amount of sulphur.

2.5 Summary

From the literature on NO_x emission studies, it can be concluded that emission levels depend on the type of engine fuel, type of engine used and various load conditions. [35] provides an insight on the effect of biodiesel on NO_x emissions. They concluded that NO_x emissions can be mitigated by modifying engine control parameters such as reduction of injection timing and increasing EGR . They maintained that more studies were necessary as there was very little commercial use of EGR [40]. In spite of a substantial number of NO_x emission studies on buses, there are limited reports of emissions studies for the running condition of buses due to various reasons such as disturbances in environmental parameters, un-availability of vehicles and inconsistencies in data collection procedures. The current literature survey found fewer number of reports on studies that considered engine parameters while the data was collected.

Numerous experiments were setup to show the effect of EGR and multiple injections on the reduction of NO_x emissions and PM. The experiments inferred that multiple injections reduced the amount of PM emissions and the combination with EGR also led to a decrease in NO_x emissions and called for real time analysis of the same. There have been a small number of studies comparing the NO_x emissions and PM emissions in both EGR and NON-EGR buses with real-time data collection. In order to meet emission standards and to safeguard the environment, control strategies involving various engine conditions and the emission levels are required.

Chapter 3

Methodology

3.1 Problem Definition

The primary objective of this research was to employ real-time data collection in the running conditions of a bus on its route to ascertain the NO_x emission values with respect to the engine data (rpm) and to calculate the PM and NO_x emissions values in cold idle and hot idle cases . In order to accomplish these objectives, a protocol was developed and followed that can be broadly divided into five sections:

1. Project planning
2. Experimental design
3. Data collection
4. Data organization
5. Data analysis

The following sections give a detailed view of the methodology and study design used.

3.2 Transit Bus Fleet Characteristics

Characteristics like vehicle make, model, model year, engine type and size all play a role in tail-pipe emissions. TARTA (Toledo Area Regional Transit Authority) provided vehicles on which our tests were carried out. TARTA serves nine communities with over 230 buses categorized into ten different fleets. The categorization was done based on the engine type and the manufacturing year [41].

Experimental studies were carried out on a bus with an EGR equipped engine and another bus with a NON-EGR equipped engine. All the 800 series buses in TARTA have EGR equipped engines and the 700 series buses have NON-EGR equipped engines. A 701 bus from the 700 series and an 802 bus from the 800 series were chosen to perform the experimental study. Table 3.1 summarizes the engine specifications of the transit buses tested.

Table 3.1: Engine specifications of the transit buses tested

Bus Series/Number	700/701	800/802
Engine	Cummins ISL6LTAA	Cummins ISL-07
Chassis	Gillig	Eldorado National
Year of Manufacture	2003	2010
Gross Vehicle Weight (lbs.)	39000	42760
Engine Capacity	8.9L	8.9L
Maximum Power	289HP @ 2000 RPM	280HP @ 2200 RPM
Maximum Torque	900 ft.lbs. @ 1300 RPM	900 ft.lbs @ 1300 RPM
Emission Certifications	2007	2007

3.3 Test Fuels

Understanding the effect of emission reduction on human health and the environment, TARTA has adopted alternative fuels including B20 and ULSD since June 2006. In order to maintain cost efficiency and due to the unavailability of B20 fuel, TARTA has switched to B5 grade biodiesel in the last couple of years. The two fuels used are obtained from certified producers, Peter Cremer and Amoco fuels.

Ultra-low sulfur NO.2 Amoco diesel fuel meets the EPA on-road requirements for sulfur content and conforms to ASTM D-975 diesel fuel specifications. To ensure good storage stability, the fuel is properly blended and suitable additives are used. Peter Cremer supplies 99.9% biodiesel and 5% of this 99.9% biodiesel is used by TARTA as B5, by mixing it with 95% of ULSD as base fuel. The 99.9% biodiesel meets EPA requirements and qualifies for ASTM D-6751 (EPA-4627) fuel specifications. In this study, B5 grade biodiesel is used. A summary of the fuel properties is provided in Table 3.2.

Table 3.2: Properties of biodiesel and ULSD

Property	**Biodiesel (B99.99%)**	**ULSD**
Cetane Number	47	40
Cloud Point (Summer)(°F)	-	20
Cloud Point (Winter)(°F)	42.8	15
Flash Point(°F)	>320	125
Sulfur (ppm)	<1	15
Water & Sediment (moisture) (Vol. %)	<0.005	0.05
Kinematic Viscosity, 40°C (mm^2/sec)	4.31	1.9-3.4

3.4 Test Route

The 22F number route was selected for this study as it is the longest route in the city of Toledo. The NO_x emission data was collected for the route, which started from Franklin Park Mall and ended at Jefferson Street, with a testing time for each run of approximately 70 minutes, which included 35 minutes from Franklin Park mall to Jefferson Street and 35 minutes from Jefferson Street to Franklin Park Mall. There were 25 traffic signal points and several TARTA bus stops on this route. A diagrammatic view of the test run route is shown in the Fig. 3.1

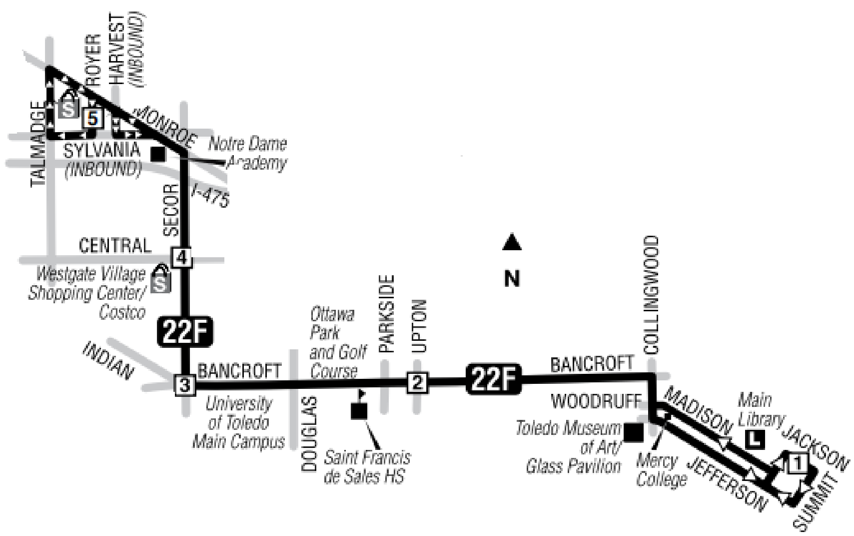

Figure 3-1: Route map of the test run

The running condition data was collected on both the EGR and NON-EGR buses plying on this route. Data collection for hot idle and cold idle modes was conducted in the garage. In order to avoid the influence of other parameters on data collection, the procedure was conducted in an open area outside the garage.

3.5 Experimental Study Design

Preparation for field data collection involved three major elements

1. Coordination with the division of TARTA management regarding scheduling of the test and access to the buses

2. Verification of the status of the Portable Emissions Measurement System (PEMS)

3. Availability of all necessary accessories and complete data collection.

The most critical factor was to communicate with the officials on specifications of the buses to be tested, the date and time they were to be tested, the fuel type used, duty cycle performance and the location of the buses for comfortable data collection. This field study involved data collection of NO_x and PM emissions from the transit buses.

The collection of data was carried out in three stages namely cold idle mode, hot idle mode and the running conditions of the buses. Cold idle mode is the phase in which the data is collected in the morning before the buses left the garage. In this condition, the acceleration of the bus was zero, and the load was almost negligible. In the running bus conditions, data was collected when the bus was in motion. The running bus condition was divided into four different modes: deceleration mode, acceleration mode, variable speed mode and partial idle mode.

The deceleration mode was the time taken from the time the buses started decelerating to the time they reached the idle position. Acceleration mode included the time taken for the buses to start from an idle position and the time it takes to attain a constant speed. Due to the busy traffic, the buses stopped. Also, due to various other road conditions, the buses moved with variable speeds accordingly and this data was considered the variable speed mode. The idle times attained at the traffic signals, stop signs and at the designated bus-stops attributed to the partial idling mode.

Factors such as payload, acceleration, deceleration, road traffic, traffic signals and the road conditions affected the amount of NO_x emissions. Lastly, the hot idle mode data was collected when the buses arrived at the garage after they finished their

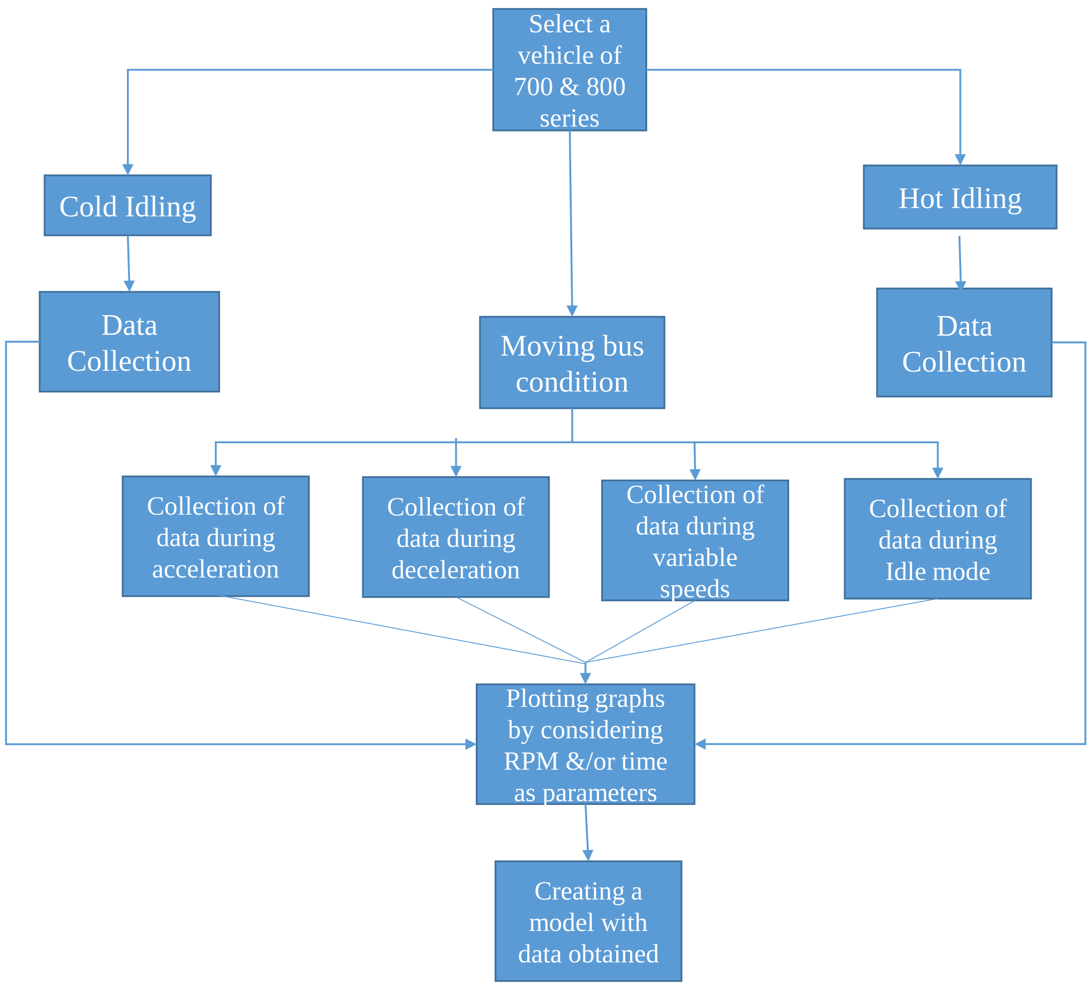

Figure 3-2: Flowchart for the collection of NO_x emission data

routes. The NO_x emission values were measured using a MEXA-720, Horiba NO_x analyzer. The Cummins insite 6 software program and the equipment involved was connected to a laptop to collect the engine data. Fig. 3-2 shows the data acquisition scheme for collecting the NO_x emissions data.

Collection of PM data was similar to that of NO_x emissions data collection. This data was collected at cold idling and hot idling conditions. Sampling was done by using a CATCH CAN instrument that is shown in Fig. 3-5.

The above mentioned protocols were iterated every day during the data collection process. The experiments were conducted on the same buses throughout the collection process so as to maintain the same engine conditions. Owing to the large fleet of buses and various routes, it was difficult to schedule the same buses for emission testing. Such constraints contributed to the delay in the experimental part of the project.

3.6 Instrumentation

The portable emission measurement system used to collect tail pipe emissions in this study is the MEXA-720 Horiba NO_x Analyzer system manufactured by Horiba Inc. This analyzer is light, compact and contains a zirconia-ceramic sensor. The single unit provides fast response measurements of NO_x concentrations from diesel or lean-burn engines. The sensor can be directly inserted into the tail pipe to collect NO_x emission data and eliminates the need for a sample-handling unit. The experimental setup of the instrument inside the bus is shown in the Fig. 3-3.

Figure 3-3: Instrument setup inside the bus

The specifications of the Horiba NO_x analyzer are represented in Table 4.2.

In order to gather the different engine parameters such as rpm, engine temperature, exhaust gas pressure, EGR temperature Cummins insite 6 software along with the toolbox was used. For the 800 series bus, one end of the 9 pin plug connector is connected to the laptop through USB and the other end is connected to the on

Table 3.3: Specification of MEXA 720 Horiba NO_x analyzer

Component	**NO_x**
Ranges	0-3000 ppm
Accuracy	0-1000 ppm: ±30 ppm with 3 point calibration; 1001-2K ppm: ±3% of reading with 3 point calibration
Warm-up time	Approximately three minutes after turned on
Sample gas	Stoichiometric to lean for diesel or lean-burn engines
Conditions	Measurement gas temperature: -7 to 800°C
Ambient conditions	For main unit: 5 to 45 °C; (operating), -10 to 70 °C (storage) Less than 80% relative humidity

board diagnostic unit (OBD) in the bus. Similarly, for the 700 series bus a 6 pin plug connector was used. The Fig. 3-4 shows a Cummins 9 pin plug connector.

An aluminum attachment designed to shield the instrument analyzer from the heat and to ensure uniform insertion depth of the probe into the vehicle exhaust and to keep it intact during the running condition. Continuous power supply was ensured to both the instruments and the laptop to avoid interruptions in data collection.

The particulate matter data collected was sampled by fixing a quartz filter paper of 12 cm in diameter to a Catch Can which was placed inside the exhaust pipe to capture the emissions. Fig. 3-5 shows the CATCH CAN and the quartz filter paper used to collect particulate matter data.

PALL flextissuquartz 2500 membrane quartz filters were used for the field experiments which a have a retention rate of 99.9% for PM of size 0.3 (micro) meters. Prior to sampling, these filter papers are stored in vacuum desiccators for 24-72 hours to

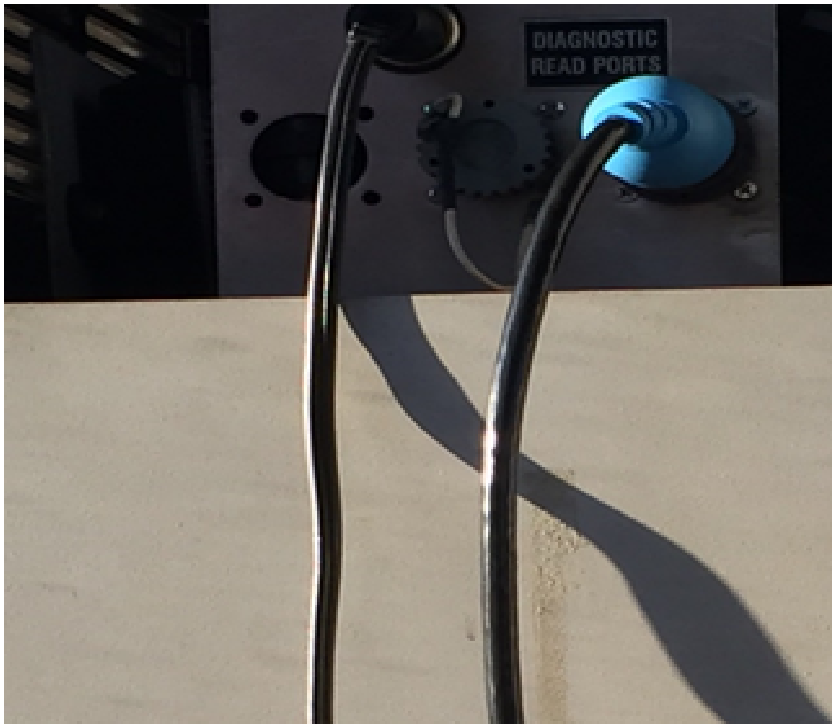

Figure 3-4: Cummins 9 pin plug connector

equilibrate the filters and are then weighed using gravimetric mass balance. After PM collection, these filters are calibrated and gravimetrically weighed again. The difference in weights before and after the collection of PM matter gives the amount of PM collected.

Figure 3-5: (a) Blank quartz filter paper (b) CATCH CAN instrument (c) Quartz filter paper after sample collection

3.7 Data Collection

Installation of the equipment on the bus was carried out in the garage on the day of testing. It took around 20 minutes for installation and 15 minutes for the removal of the setup from the bus. Care was taken during the removal of equipment from the bus since the equipment was too hot to touch. The experimental setup of the instrument is shown in the Fig. 3-6.

The cold idling data was collected at 4:30am every morning just before the bus left the garage and the hot idling data was collected after 10:45 pm when the bus returned to the garage after completing its route. The same bus was used to collect the cold idling and hot idling data. The data was collected over a period of twelve days for the 701 bus and 802 bus respectively. The first half of the data collection days were used to collect NO_x emission values whereas the second half of the data collection was used to collect PM samples. The engine performance data and the emission data were collected simultaneously without any time lag. Second by second data of NO_x emissions was collected along with the engine performance data.

In the running bus condition, the experiments were conducted for 8 days each on the 701 and the 802 bus. All the tests were performed on weekdays.The bus would leave the TARTA garage at 7:25 AM in the morning and return to the garage by

Figure 3-6: Instrument setup outside bus

10:30 AM after finishing the route.

The recorded data from the different modes of the running condition along with its corresponding engine parameters (rpm), were transferred and recorded on an Excel sheet. The NO_x emission data was collected with respect to rpm values.

Data collected during any interruptions for instance, malfunctioning and slipping of instruments due to road conditions and sudden braking, was not considered and test was determined as a fail test. All the data obtained from the successful tests was used for analysis. The instrument was calibrated just before the data collection, hence the data obtained is assumed to be free from errors and all the data has been used for statistical analysis.

3.8 Data Analysis

The NO_x emission data collected was analyzed using regression techniques. Three different regression techniques were implemented to compare the efficiency of the prediction of NO_x values. Random Forest Regression (RFR) and Support Vector Machine Regression (SVMR) in addition to the Levenberg Marquardt (LM) algorithm [42] were used here.

ANN techniques have emerged as a powerful tool, capable of modeling non-linear data with ease. The individual units (called neurons) are inter-connected with neurons of other layers using weighted links. For supervised ANNs, the network parameters, like weights and biases, are updated using different algorithms that make use of the error signals, where the error is the difference between the desired output and the current network output. Multi-Layer Perceptron (MLP) networks are most popularly used ANNs. MLP constitutes of input, hidden and output layers and can have more than one hidden layer.

Under-learning occurs when the network does not learn the training data, thus gives large errors. On the other hand, over-learning is a situation where the network over-learns the training data resulting in it failing to capture the inherent relationship between input and output i.e., it fails to generalize the model.

The desired output is represented as y_k, and Y_k is the predicted output and is given by:

$$Y_k = \sum_{(j=1)}^{p} [(Z_j * V_{jk}) + V_{0j}]$$

where,

$$Z_j = (1 + e^{-(\sum_{(j=1)}^{p} \sigma_j)})^{-1}$$

$$\sigma = \sum_{(i=1)}^{n} (X_i(u_{ij}) + p_{0i})$$

As shown in Fig. 3-7, n is the number of input neurons and, p and q are number of hidden and output neurons respectively. V_{0q} represents the q^{th} neuron bias weight parameter in the output layer. The weight link between the hidden layer p^{th} neuron and output layer q^{th} neuron is given by V_{pq}. The output of the p^{th} hidden neuron is represented by z_p, where $\sigma()$ is the activation function of the hidden neuron. x_i is the n^th input neuron, u_{np} is the weight link between the p^{th} hidden neuron and n^{th} input neuron and u_{0p} is the p^{th} hidden neuron bias parameter.

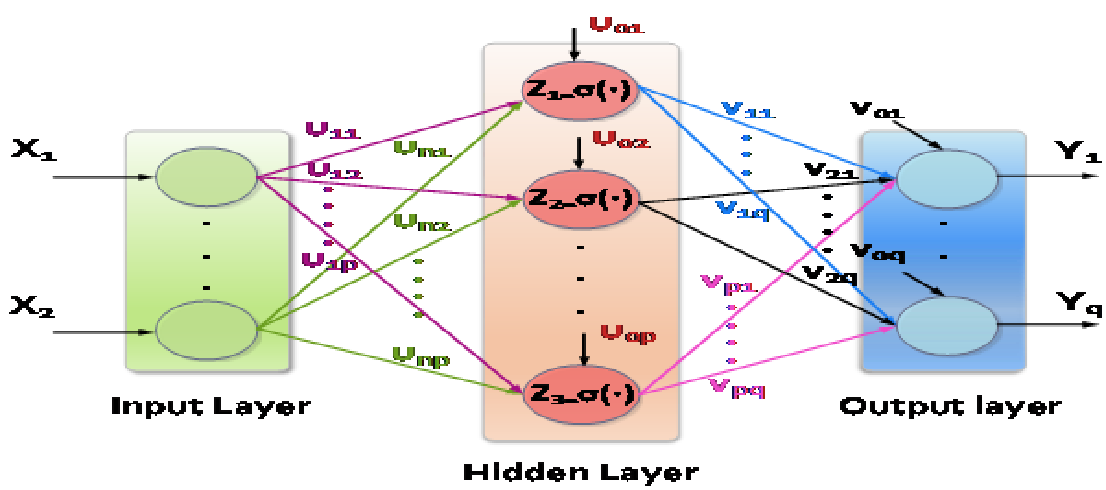

Figure 3-7: A MLP ANN with 3 layers

The Levenberg-Marquardt (LM) method is a standard technique used to solve nonlinear least squares problems. The algorithm was first published in 1944 by Kenneth Levenberg, and was rediscovered in 1963 by Donald Marquardt [43]. The LM curve-fitting method is actually a combination of two minimization methods: the steepest descent method and the Gauss-Newton method. In the steepest descent method, the sum of the squared errors is reduced by updating the parameters in the steepest-descent direction. In the Gauss-Newton method, the sum of the squared errors is reduced by assuming the least squares function is locally quadratic, and finding the minimum of the quadratic [42].

Random Forest, proposed by [44], is a robust and flexible classification and regression tree method used for modeling the input-output functional relationship appropriately. Individual Regression trees are constructed using bootstrap samples from the training data and the ensemble of these individual trees is called a Random Forest. Each tree acts as a regression function on its own, and the final output is taken as the average of the individual tree outputs. Moreover, due to the RFR built-in cross validation capability carried out with the help of out-of-bag samples, it provides a realistic prediction error estimates during the training process, and hence, it is suitable for real time implementation [45]. Furthermore, unlike neural networks (NNs), RFR handles the high dimensional data effectively [46]. RFR is applied in many fields such as classification in ecology [47], Gene selection and classification of microarray data [48], predicting customer retention and profitability [49] etc.

The random forest trees predict Y, a response variable, by estimating the mean of the conditional distribution of Y and X, a high-dimensional predictor variable. The estimation of conditional mean is done by minimizing the expected squared error loss as given by Eq. 3.1.

$$E(Y/\bar{X} = x) = arg\min_{T} E((Y - \bar{Y})^2 | \bar{X} = x) \tag{3.1}$$

where, X and Y are real valued predictor and response variables respectively, and $\hat{Y}$ is the estimate of the response variable.

RFR is a non-parametric regression approach. It consists of a set of N (user defined number) trees R1 ($\bar{X}$), R2 ($\bar{X}$) ... RN ($\bar{X}$), where $\bar{X} = x_1, x_2..., x_p$ is a p-dimensional input vector that forms a forest. The ensemble produces N outputs corresponding to each tree, Y1 $=$ R1 ($\bar{X}$) ... Yn $=$ Rn ($\bar{X}$) ... Y$\hat{N}$ $=$ RN ($\bar{X}$), where Y$\hat{n}$, n= 1, 2,.. N, is the nth tree output. The final output $\bar{Y}$ is an average of all tree predictions for that input.

For each regression tree construction, a bootstrap sample is drawn, with replacement from the original training set. A total of two-thirds of the samples of the new training sample are utilized for construction of trees, and one-third of the sample is left out and this data becomes the out-of-bag sample. Hence, each time a regression tree is constructed using randomly drawn training sample from the original dataset; an out-of-bag sample can be used to test its accuracy. This inbuilt validation feature improves the generalization capability of the Random Forests when an independent test data is utilized [44].

Support vector machines had been initially introduced to simplify solving pattern recognition problem. In this method, the data is mapped into a higher dimensional input space and an optimal separating hyperplane is constructed. In order to minimize the VC dimension, kernel functions and parameters are chosen. Recent studies show that SVM's have been applied to radial basis functions and multilayer perceptron [50].

SVR is used in a variety of applications that require regression analysis. A trained SVR approximates a non-linear regression function that maps from an input object to a real number. The most commonly used versions of SVR are 'ε-SVR' and ν-SVR'. ε and ν are two different parameters used to apply a penalty to optimize points that are not accurately anticipated. In the parameter ν (0, 1], support vectors lie under the lower bound and the badly predicted errors lie under upper bound. The parameter ε can take any positive value. Thus the additional bound in ν-SVR gives a more meaningful interpretation than ε-SVR [51]. For this reason ν-SVR is selected for verifying the effectiveness of the proposed QRF-based integration algorithm. Recently, SVR has been applied in modeling and estimation of MEMS sensors thus demonstrating that ν-SVR performs better than ANN [52].

Since ν-SVR has more meaningful interpretation than ε-SVR, ν-SVR is employed in this paper for approximation of the non-linear regression function,

$$f(x) = w^T * \phi(x) + b \tag{3.2}$$

where w^T is the weight vector to the corresponding non-linear mapping function ϕ(x), which maps the input space to a higher dimensional space, and b is a bias. The parameters w and b need to be estimated in order to approximate the non-linear regression function, such that the function f(x) and the desired output should be as close as possible.

To analyze the particulate matter samples which were collected, EDS analysis and ICP-MS was carried out. The instrument used for EDS analysis was Oxford Instruments EDS X-Max $50mm^2$ / FEI Quanta 3D FEG Dual Beam Electron Microscope. The following conditions were used spectrum range (0-10 kEV) and detector (X-Max). The samples were prepared as follows: resin flakes were placed on double side carbon tape then attached to aluminum stubs. The samples were then coated with gold using the sputter coater unit (Cressington 108 auto) for 30 seconds. Subsequently, sample stubs were loaded in the SEM and examined in the EDS.

The instrument used for ICP-MS was the Xseries 2 (Thermo Scientific, MA, USA). The procedure for ICP-MS analysis was as follows: approximately 200 mg of each sample were digested in HNO3 using a CEM Mars microwave. For digestion the conditions were as follows power (100%), ramp (15 min), pressure (800 psi), Temperature (210°C), and holding time (15 minutes). After digestion, samples were filtered to remove particulate material. The filtrate was then diluted to 3.5% HNO3 for analysis. For quantitative analysis, standards and internal standards were prepared by using the certified ICP-MS standards from Inorganic Ventures. Correlation coefficients for calibration curves were above 0.999. Trace metals determined in the solutions were reported in micrograms per gram (μg/g) of sample.

Chapter 4

Results and Discussion

4.1 Analysis of NO_x Emission data

This research involved elaborate real-time measurement of NO_x and PM with many operational and traffic variables that had effects on the emissions of public transport buses. This chapter interprets the results of the NO_x emissions and particulate matter samples obtained from the public transport buses running on biodiesel.

The first section of the Chapter deals with field data presentation and regression model analysis of NO_x emission data. It includes the results of NO_x emissions obtained from idling/acceleration/variable speed motion/deceleration conditions along with the various engine parameters. These results were tabulated and compiled for both EGR and NON-EGR equipped engine transit buses. The second section includes the results obtained from the elemental analysis on the PM samples. The results were obtained from the analysis involving ICP-MS, energy dispersive X-ray spectroscopy (EDS) and scanning electron microscopy (SEM).

4.1.1 Idle Condition

The values were collected for both EGR and NON-EGR engine buses. These buses were tested in both cold idling and hot idling conditions. The cold idling values for an

EGR engine bus were found to be 30% lower than that compared to the NON-EGR equipped bus as seen in Fig. 4-1.

The hot idling values for an EGR engine bus are noted to be 15-20% lower than a NON-EGR engine bus as seen in Fig. 4-2. As already stated in Chapter 3, both buses run on the same type of fuel, were tested on the same routes and in the same driving conditions with negligible changes in load. This clearly shows the effect of exhaust gas recirculation in an engine.

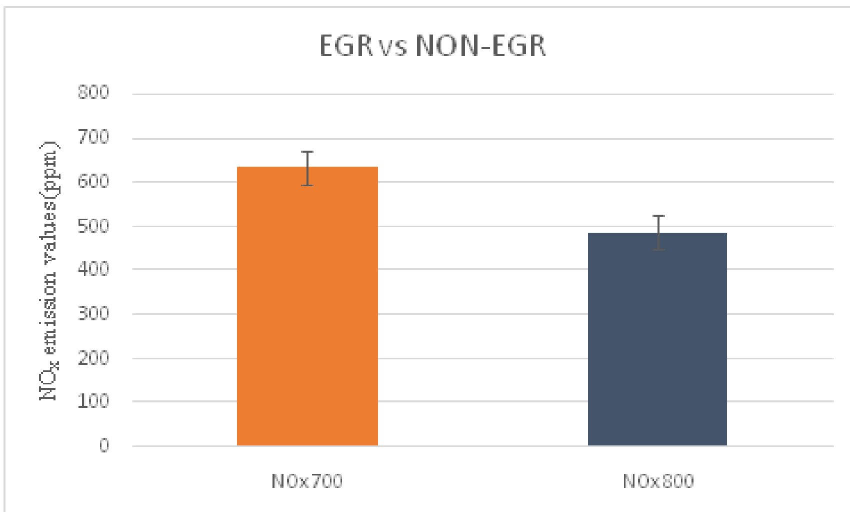

Figure 4-1: Cold idling values of EGR and NON-EGR engine buses

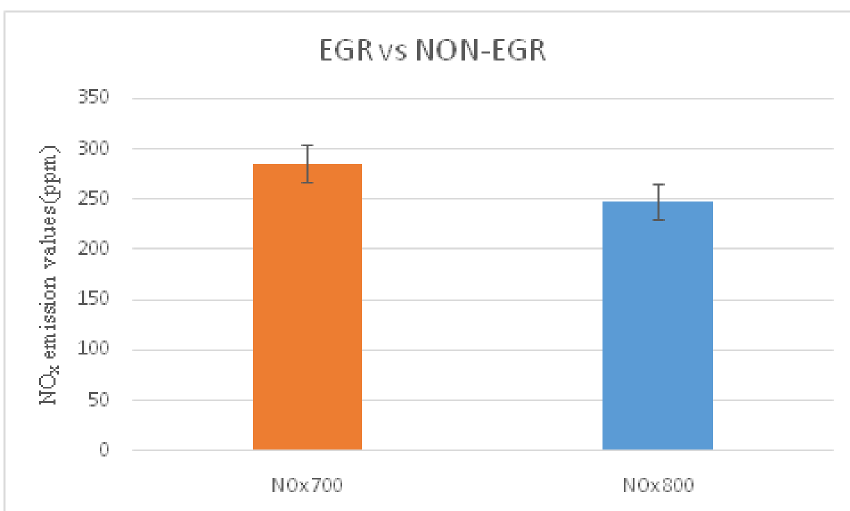

Figure 4-2: Hot idling values of EGR and NON-EGR engine buses

The NO_x emission data were collected from a Horiba NO_x analyzer. From the literature review, the data collected for 15 minutes reached an optimum value in the cold idling case where-as it took 10minutes to reach a constant value in the hot idling case as the bus was running all day. The Horiba NO_x analyzer measured the emission data on a second to second scale. As mentioned in the methodology, the data were collected for 900 seconds over a period of six days continuously on the each bus and the average was taken. This process is known as average time concentration and all the idling datasets were obtained and represented in this method.

The emissions from the cold idling engine were seen to be comparatively higher and there was 25-30% higher emissions for the NON-EGR engine bus when compared to the EGR engine bus as seen in Fig. 4-3. Due to the fact that the hot idling values were collected after the bus ran for an entire day, the hot idling data converged faster and were seen to be lower than the cold idling condition. The difference between the EGR and the NON-EGR engine buses ranged between 14-20% as seen in Fig. 4.4.

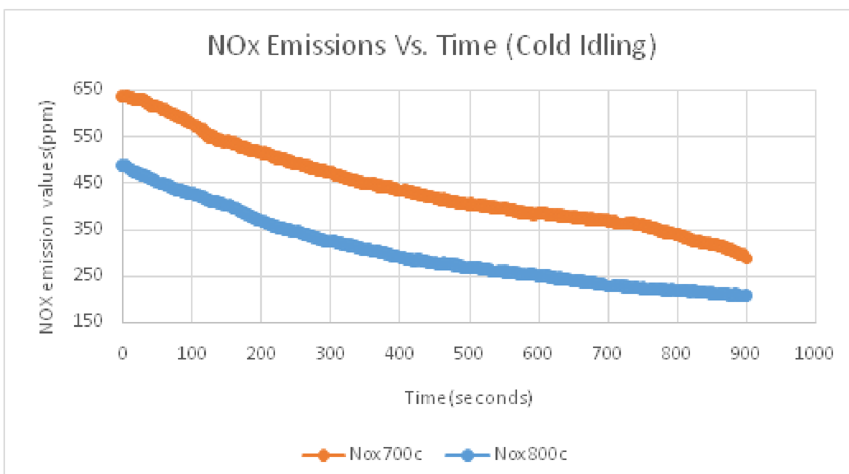

Figure 4-3: NO_x emissions in Cold Idling

Table 4.1: Engine parameters: NON-EGR engine bus (700 series)

Engine Parameters	**700 Cold Idling Conditions**		**700 Hot Idling Conditions**	
	Maximum	Minimum	Maximum	Minimum
Engine Temperature(°F)	213.9	145.6	269.3	236.1
Exhaust Gas Pressure(mmHg)	48.6	40.9	42.3	34.6
Fuel Flow Rate Command(gph)	4.2	2.4	3.2	1.7
NO_x Emissions(ppm)	635	289	286	201

Table 4.2: Engine parameters: EGR engine bus (800 series)

Engine Parameters	**800 Cold Idling Conditions**		**800 Hot Idling Conditions**	
	Maximum	Minimum	Maximum	Minimum
EGR Temperature(°F)	139.6	81.9	93.4	69.7
Diesel Oxidation Catalyst Intake Temperature(°F)	278.7	210.8	214.7	173.4
Diesel Particulate Filter Intake Temperature(°F)	241.7	189.3	195.2	148.7
Diesel Particulate Filter Outlet Temperature(°F)	239.4	106.5	127.3	76.4
Fuel Flow Rate Command(gph)	3.6	2.1	2.5	1.2
NO_x Emissions(ppm)	487	206	248	151

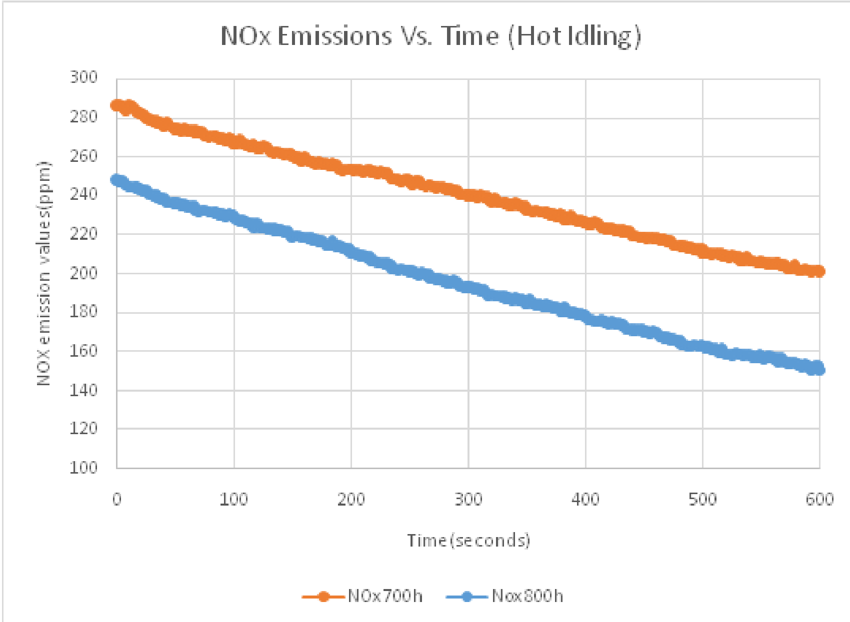

Figure 4-4: NO_x emissions in Hot Idling

4.1.2 Running Conditions

In the running condition, instantaneous concentration data-sets were developed and considered. RPM was the only engine parameter considered as it showed an effect on NO_x emissions. Both the emission data and rpm data values were noted for 8 different days. All the experiments were considered on both the fleets of buses using the same type of fuel and running on the same driving routes and conditions. The running condition of the bus was split into 4 different cases as discussed earlier. The reason for the undulations in Fig. 4.5 and 4.6 is due to the real-time fluctuations of the parameters such as road conditions, traffic signals, air condition load and different weather conditions which cannot be controlled.

In the acceleration case, the highest amounts of NO_x emissions were obtained. The difference between the EGR and the NON-EGR engine buses were noted to be about 34% as seen in Fig. 4-5.

From Fig. 4-6 and 4-7, it can be noted that NO_x emission values decreased with a decrease in rpm and vice versa. It can also be noted that the NON-EGR engine buses had higher emission rates than the EGR engine buses. For the 700 series bus, the maximum NO_x emission value noted was 634 ppm at 2095 rpm and the minimum was 408 ppm at 1735 rpm. Similarly for the EGR engine bus (800 series), the maximum NO_x emission value noted was 472 ppm at 2064 rpm and the least was determined as 331 ppm at 1717 rpm. The passenger load was also taken into account but showed negligible effect on the NO_x emissions.

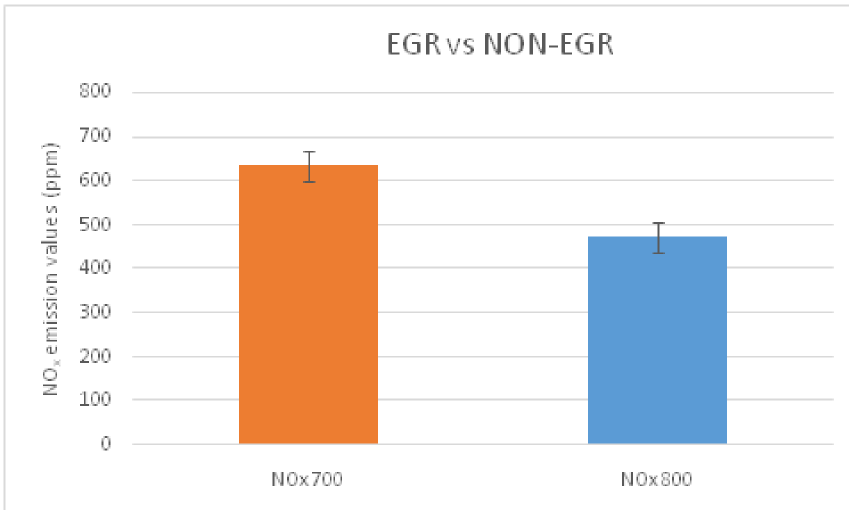

Figure 4-5: NO_x emission values(in ppm) for the two fleets of buses considered

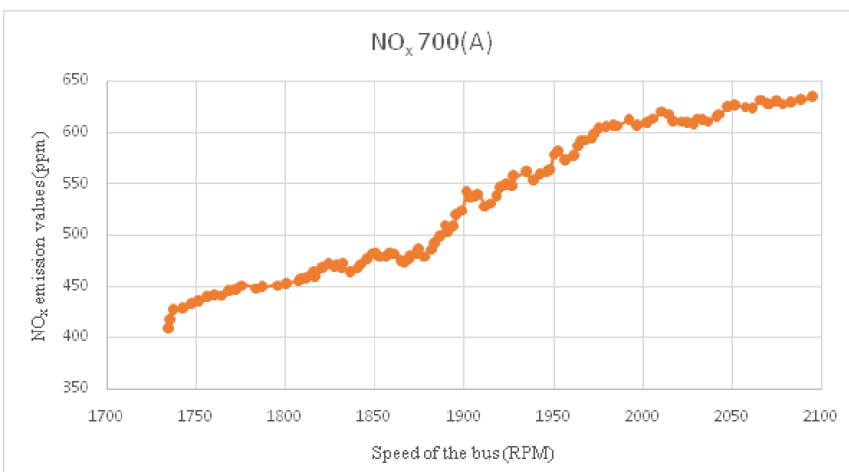

Figure 4-6: NO_x emission vs RPM for the 700 series NON-EGR engine bus

In the motion with variable speed case, the data set pertaining to the variable

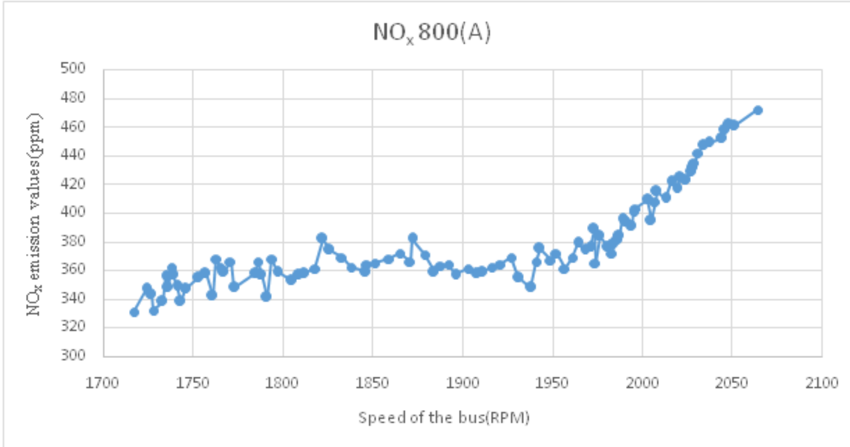

Figure 4-7: NO$_x$ emission vs RPM for the 800 series EGR engine bus

speed case is the largest of all data collected as the bus moves with variable speeds for the most part of the route. As the buses was not in the acceleration mode, the NO$_x$ emission values were noted to be slightly lower. The values obtained were in the range of 190 to 340 ppm where the highest emission value was recorded as 378 ppm at 1707 rpm for the NON-EGR engine bus (700 series) as seen in Figs. 4-8 and 4-9. For the EGR engine bus, the range was found to be between 130 to 220 ppm and the maximum was recorded as 276 ppm at 1672 rpm as seen in Fig. 4-10 respectively.

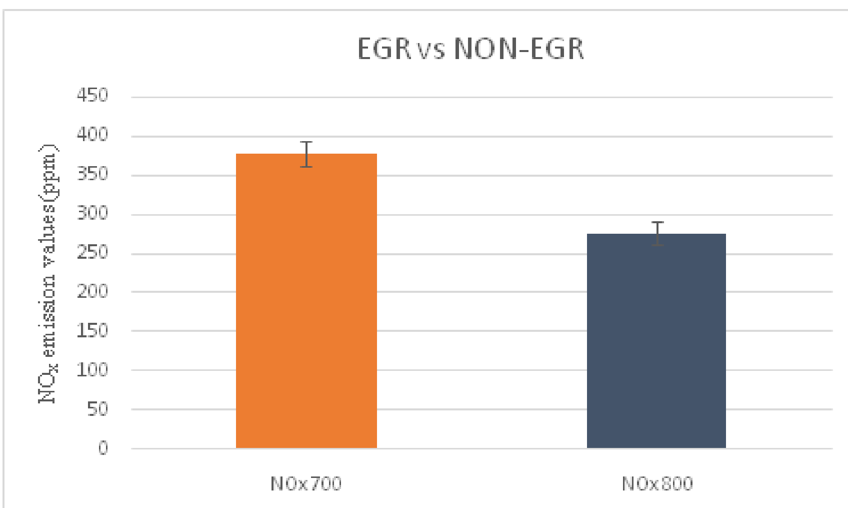

Figure 4-8: NO$_x$ emission values(in ppm) for the two fleets of buses considered

In the deceleration condition, it can be noted that there was no major difference

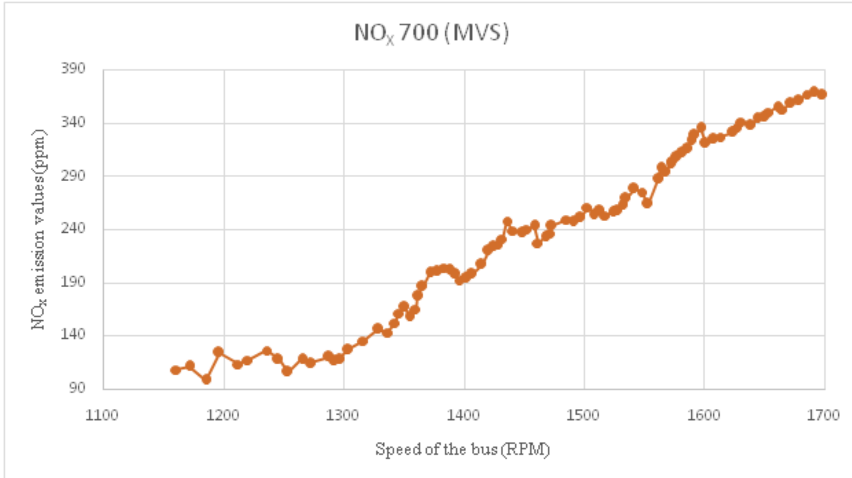

Figure 4-9: NO_x emission vs rpm for the 700 series NON-EGR engine bus

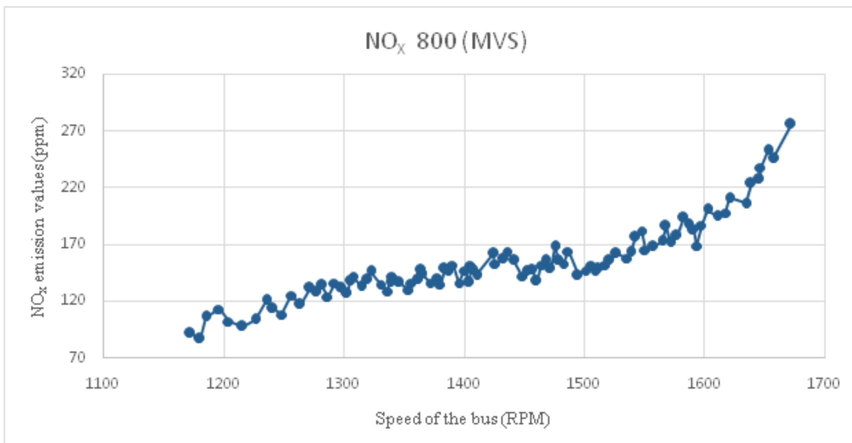

Figure 4-10: NO_x emission vs rpm for the 800 series EGR engine bus

between the EGR and the NON-EGR engine bus as the sizes of data set were small and the NO_x emissions were found to be the lowest in the deceleration case (Fig. 4.11).

From Fig. 4.12, we inferred that that the maximum NO_x emissions for a NON-EGR engine bus (700 series) was 46 ppm at an engine speed of 1204 rpm and the minimum being 14 ppm at 796 rpm. The range mostly lied between 27 and 36 ppm, respectively. Similarly, from Fig. 4.13, for an EGR engine bus (800 series), the maximum NO_x emissions was 32 ppm at 1140 rpm and the least was 13 ppm at 781 rpm and the data ranged between 17 and 25 ppm for most values of rpm.

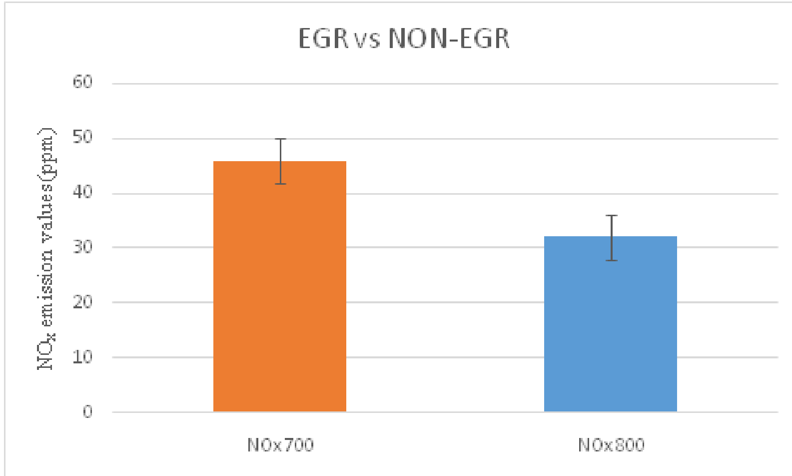

Figure 4-11: Emission values (in ppm) for the two fleets of buses considered

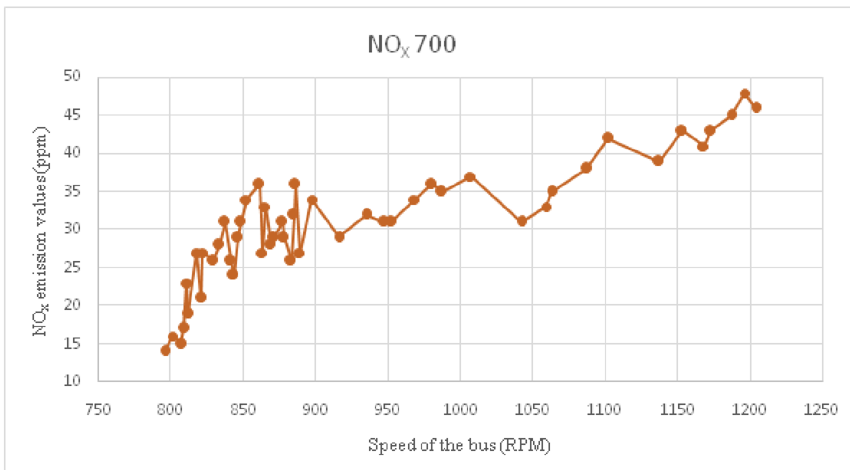

Figure 4-12: NO_x emission vs time for the 700 series NON-EGR engine bus

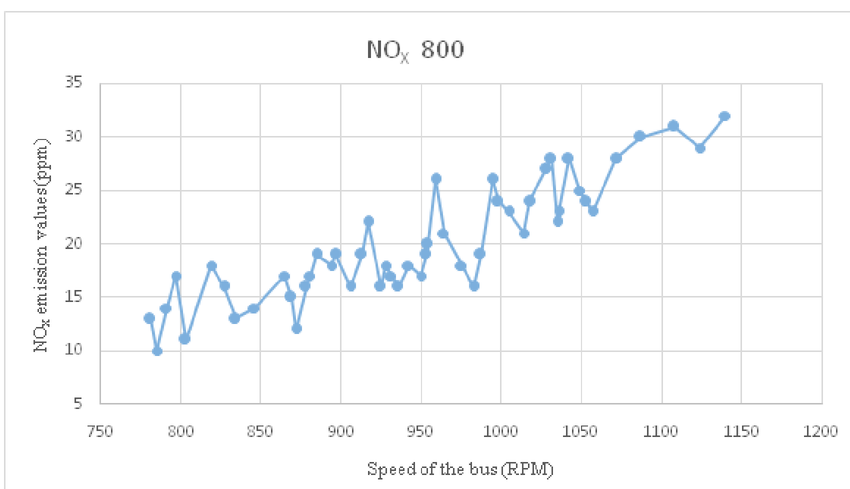

Figure 4-13: NO_x emission vs time for the 800 series EGR engine bus

The partial idling position constituted the idle positions attained at traffic signals, stop signboards and at the passenger bus stops. The partial idling time lasted about 20 seconds and therefore the readings were not as conclusive as expected due to the small timing intervals. The emissions from the NON-EGR engine bus were found to be more than 23% when compared to an EGR engine bus (Fig. 4.14). The NO_x emission values observed for a 700 series bus had a peak of 296 ppm but graduated to around 252 ppm for a time of 20 seconds (Fig. 4.15). The peak NO_x emission values for an 800 series bus, the peak value was noted to be 264 ppm and averaged to around 192 ppm over 20 seconds (Fig. 4.16).

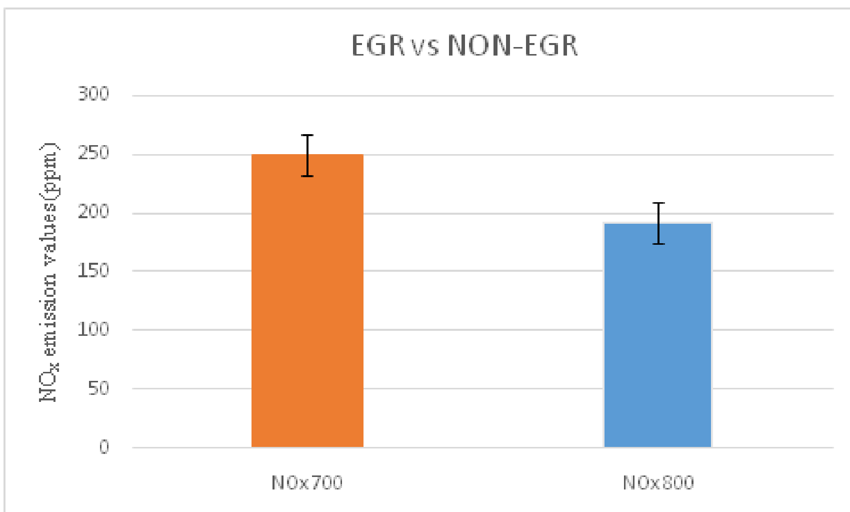

Figure 4-14: NO_x emission values (in ppm) for the two fleets of buses considered

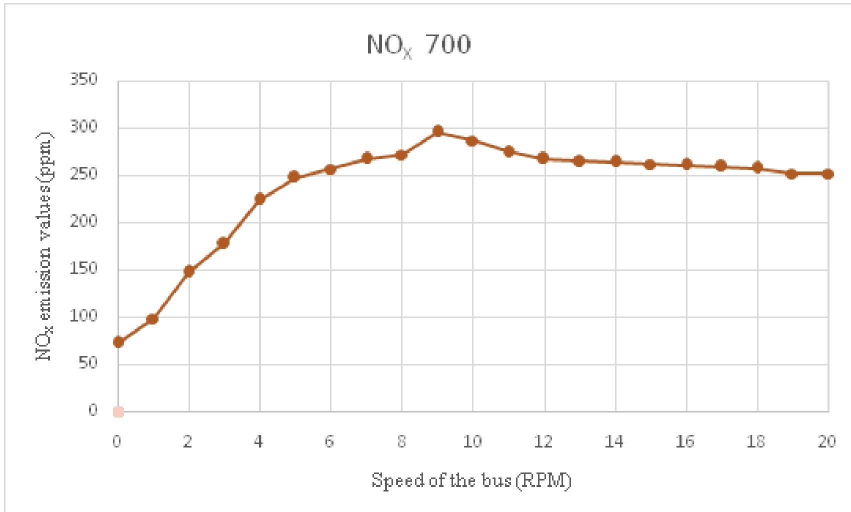

Figure 4-15: NO_x emission vs time for the 700 series NON-EGR engine bus

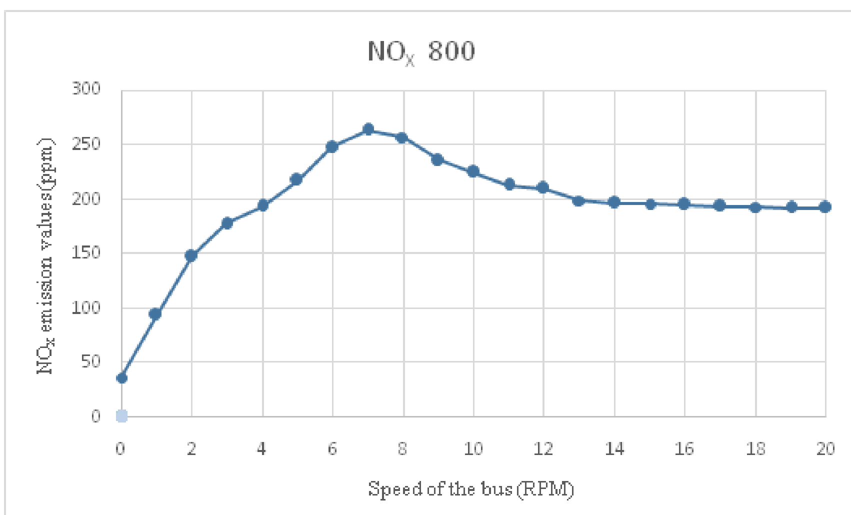

Figure 4-16: NO_x emission vs time for the 800 series EGR engine bus

4.2 Analysis of NO_x emission values using Regression Method

[53] employed the use of artificial neural network techniques for predicting NO_x emission values of urban transit buses running on biodiesel. The Levenberg-Marquardt algorithm was used on the experimental data and yielded very efficient and good model for the prediction of NO_x emission values in the cold idling condition.

To analyze the data sets obtained from the vehicular emission in this study, three different regression techniques were employed for prediction of NO_x emission values. In order to get a picture on the NO_x emission values, two new methods along with the Levenberg-Marquardt algorithm were implemented to compare the prediction efficiency of NO_x emission values. Random Forest Regression (RFR) and Support Vector Machine Regression (SVMR) techniques were employed in addition to the Levenberg Marquardt (LM) algorithm. The above methods were used to compare and determine the most efficient and powerful model for the prediction of the NO_x emission values.

The data were split into 70% training data and 30% validation data. The number of hidden neurons used differed for the cases due to the varying amount of data and ranged between 6-17 hidden neurons. Results of the five conditions are explained individually in the following section. Figs. 4.17 - 4.22 are the outputs of the ANN model, which were generated using MATLAB R2014b. In all the graphs, the blue line indicates the data predicted by the model whereas the red line indicates the actual field data. The models developed from the idle condition data sets are termed as time average concentration models and the models developed from the running conditions of the buses are termed as instantaneous concentration models. The time average concentration models are discussed in detail in the upcoming section.

4.2.1 Idle Condition

The graphs obtained from the NO_x emission prediction model for the cold idling condition using the LM, SVMR and RFR algorithms are shown in Figs. 4.17-4.22.

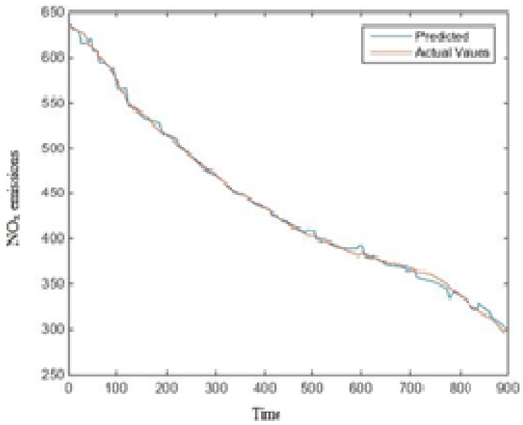

Figure 4-17: NO_x emission prediction model using LM algorithm for 700 series buses

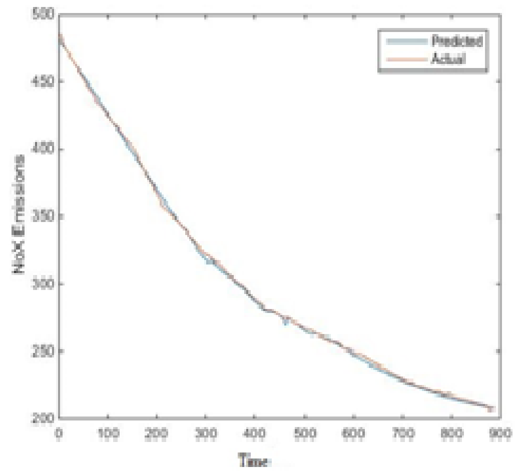

Figure 4-18: NO_x emission prediction model using LM algorithm for 800 series buses

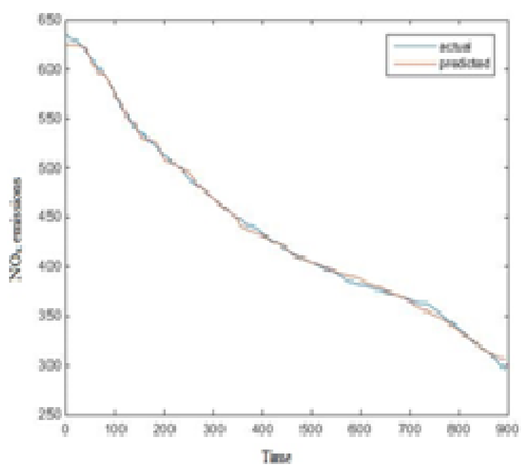

Figure 4-19: NO_x emission prediction model using SVMR algorithm for 700 series buses

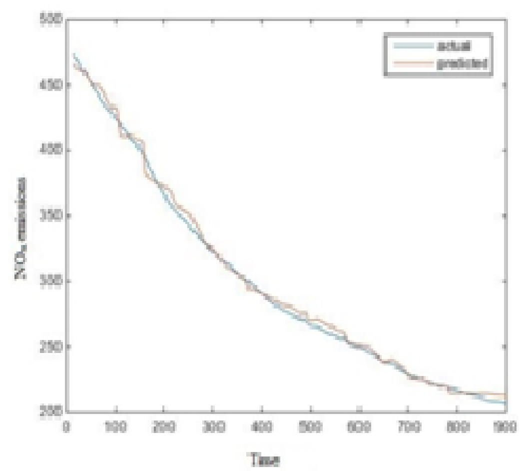

Figure 4-20: NO_x emission prediction model using SVMR algorithm for 800 series buses

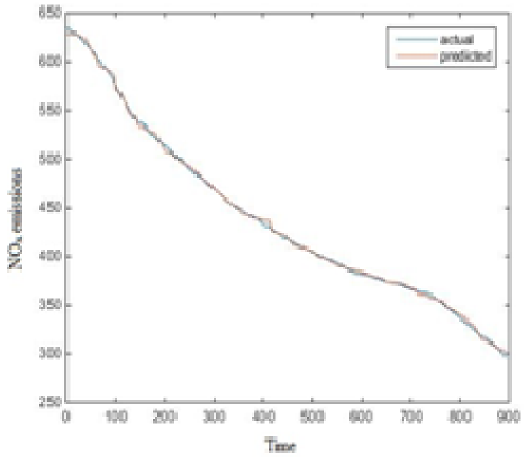

Figure 4-21: NO_x emission prediction model using RFR algorithm for 700 series buses

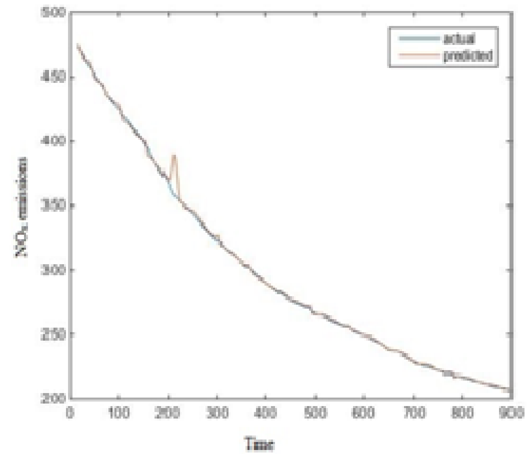

Figure 4-22: NO_x emission prediction model using RFR algorithm for 800 series buses

The error coefficients in the cold idling case are the most efficient for the 700 series bus than that for the 800 series bus while employing the RFR algorithm. The graphs obtained from the NO_x emission prediction model for the hot idling condition using the LM, SVMR and RFR algorithms are shown in Figs. 4.35 - 4.40 respectively.

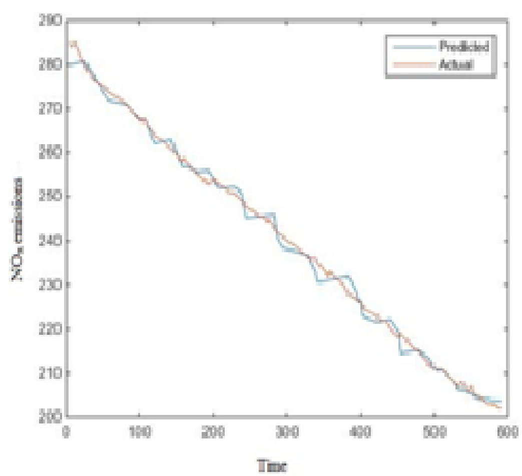

Figure 4-23: NO_x emission prediction model using LM algorithm for 700 series buses

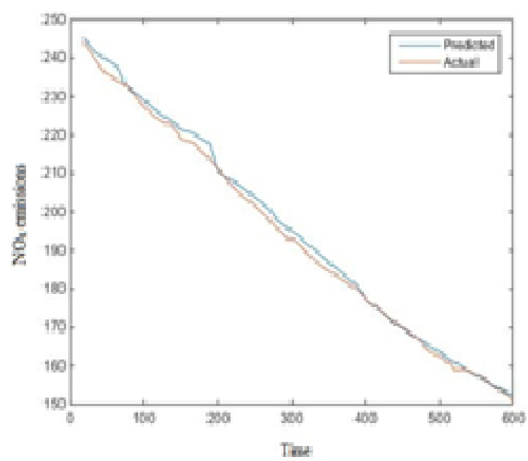

Figure 4-24: NO_x emission prediction model using LM algorithm for 800 series buses

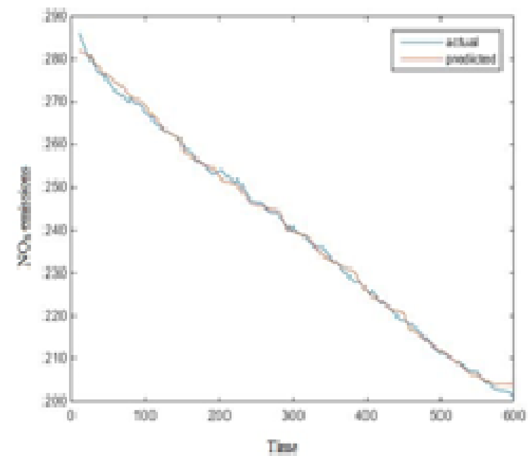

Figure 4-25: NO_x emission prediction model using SVMR algorithm for 700 series buses

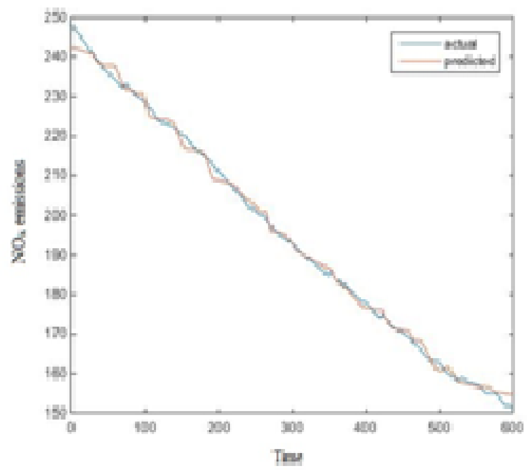

Figure 4-26: NO_x emission prediction model using SVMR algorithm for 800 series buses

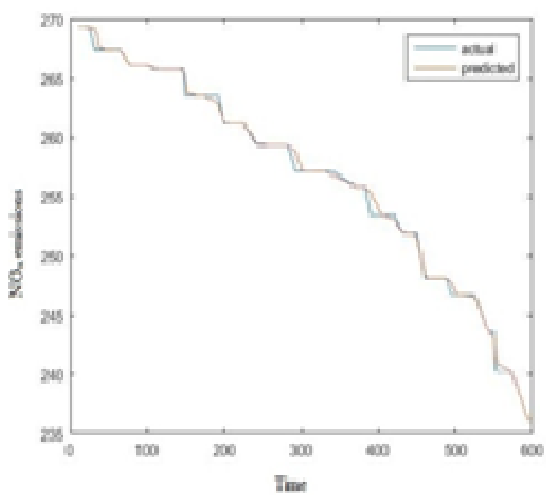

Figure 4-27: NO_x emission prediction model using SVMR algorithm for 700 series buses

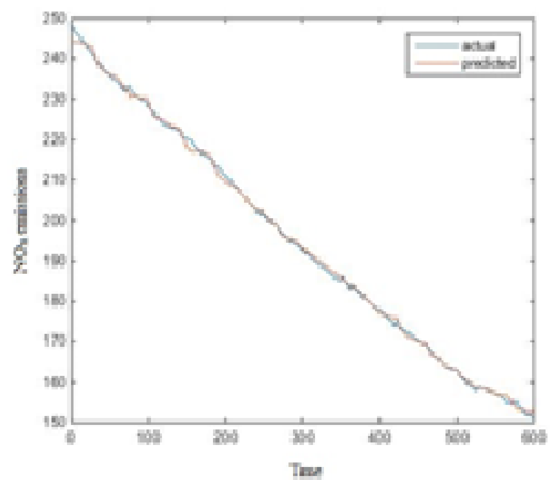

Figure 4-28: NO_x emission prediction model using SVMR algorithm for 800 series buses

The error coefficients in the hot idling case are the most efficient for the 700 series buses and the 800 series buses while using the RFR algorithm having a value of 0.9211 and 0.8625 respectively.

4.2.2 Running Condition

The instantaneous concentration models created from the regression models are explained in this section.

Acceleration analysis: The graphs obtained from the NO_x emission prediction model for the acceleration condition using the LM, SVMR and RFR algorithms are shown in Figs. 4.29 - 4.34.

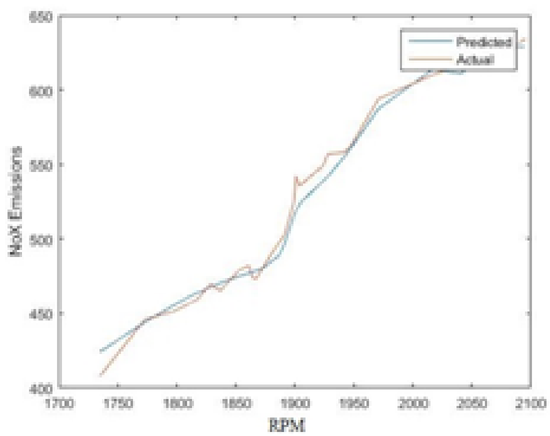

Figure 4-29: NO_x emission prediction model using LM algorithm for 700 series buses

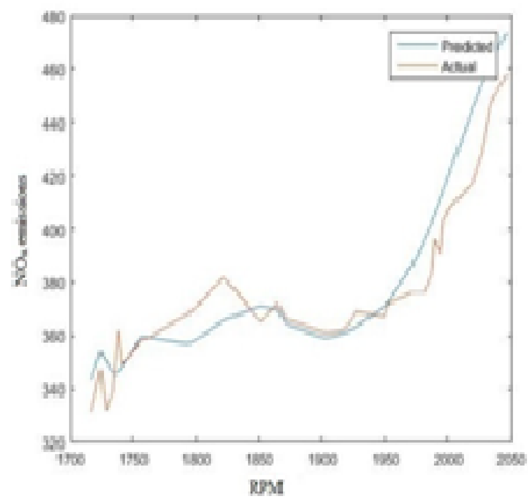

Figure 4-30: NO_x emission prediction model using LM algorithm for 800 series buses

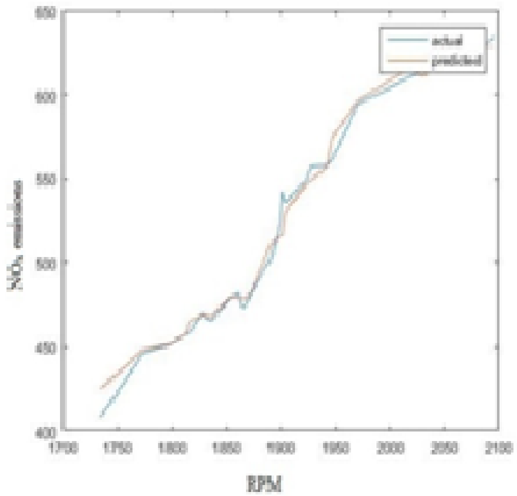

Figure 4-33: NO_x emission prediction model using RFR algorithm for 700 series buses

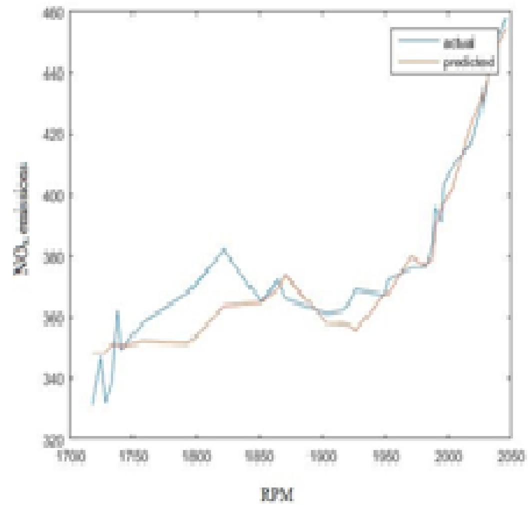

Figure 4-34: NO_x emission prediction model using RFR algorithm for 800 series buses

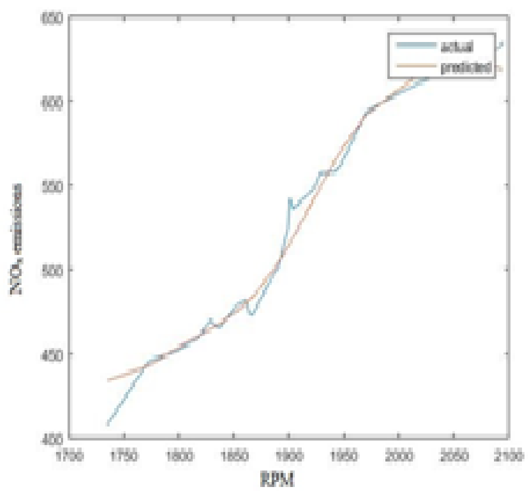

Figure 4-31: NO_x emission prediction model using SVMR algorithm for 700 series buses

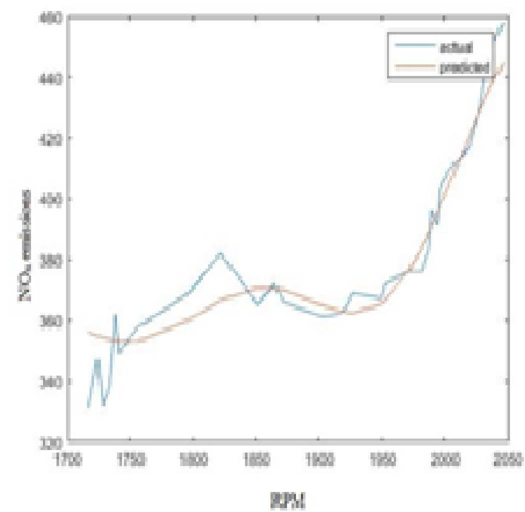

Figure 4-32: NO_x emission prediction model using SVMR algorithm for 800 series buses

The error coefficients in the acceleration case are the most efficient for the 700 series buses and the 800 series buses while using the RFR algorithm having a value of 5.08 and 6.64 respectively while using a hidden neuron number of 16.

Moving with variable speeds: The graphs obtained from the NO_x emission prediction model for the variable speed case using the LM, SVMR and RFR algorithms are shown in Figs. 4.35 - 4.40.

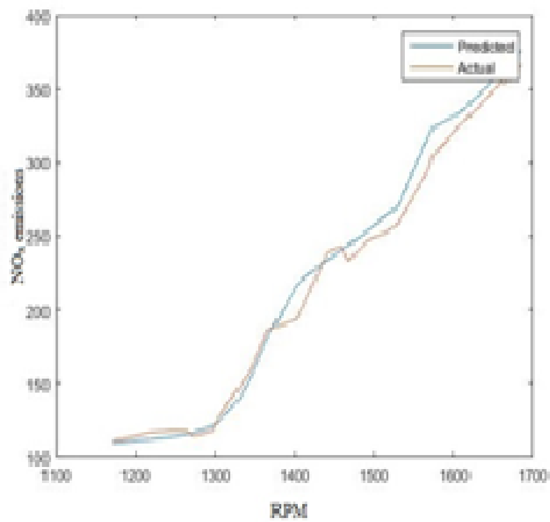

Figure 4-35: NO_x Emission prediction model using LM algorithm for 700 series buses

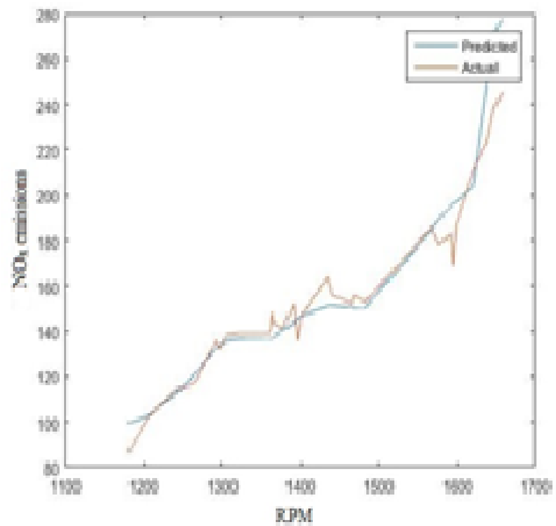

Figure 4-36: NO_x Emission prediction model using LM algorithm for 800 series buses

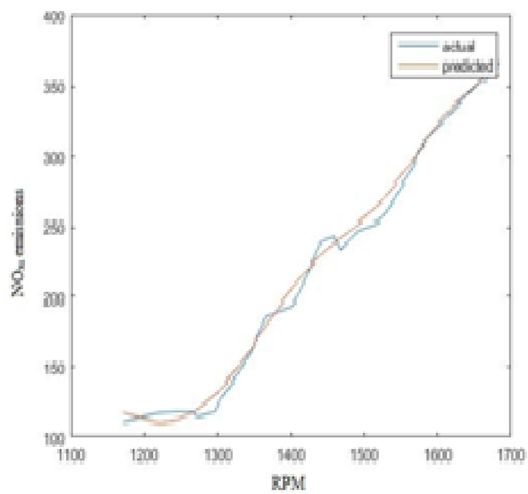

Figure 4-37: NO_x emission prediction model using SVMR algorithm for 700 series buses

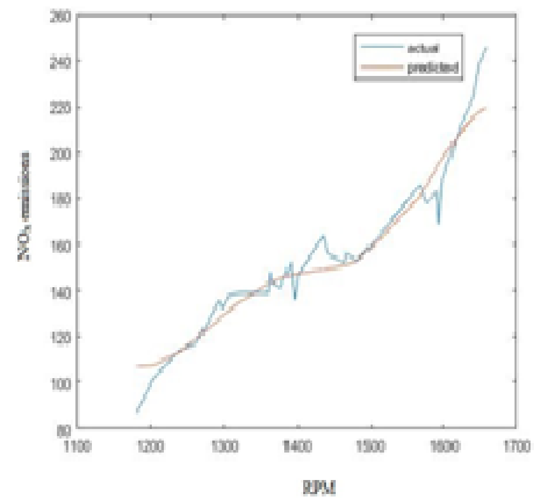

Figure 4-38: NO_x emission prediction model using SVMR algorithm for 800 series buses

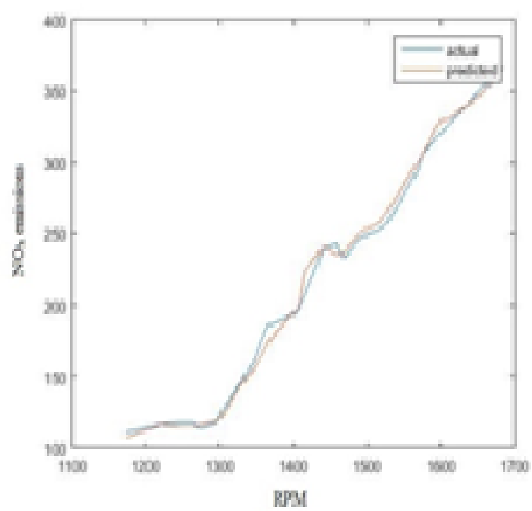

Figure 4-39: NO_x emission prediction model using RFR algorithm for 700 series buses

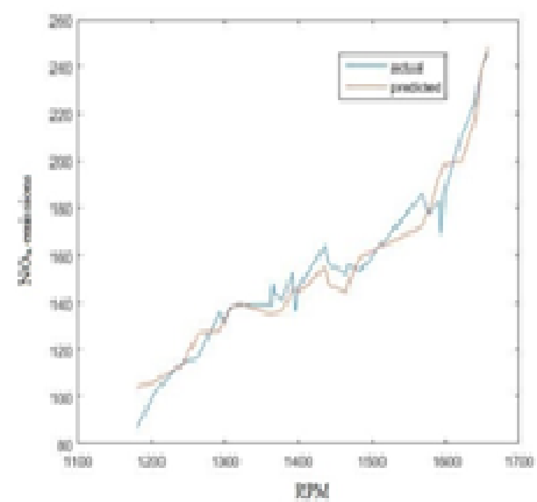

Figure 4-40: NO_x emission prediction model using RFR algorithm for 800 series buses

The best fit for the error coefficients in the moving with variable speed case for the 700 series buses and the 800 series buses are obtained while using the RFR algorithm.

4.57 and 7.37 are the respective error coefficient values for 700 and 800 series buses.

Deceleration Analysis The graphs obtained from the NO_x emission prediction model for the deceleration case using the LM, SVMR and RFR algorithms are shown in Figs. 4.41 - 4.46.

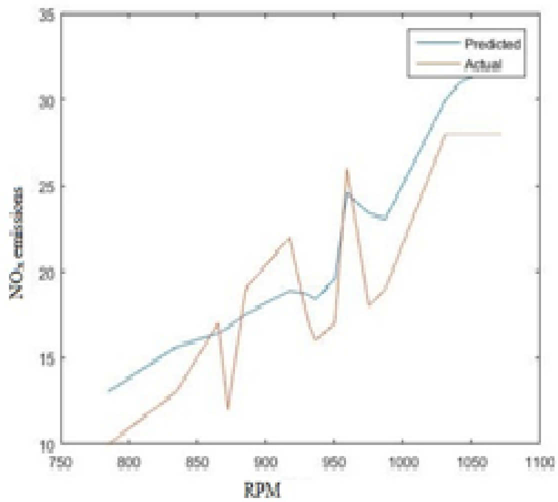

Figure 4-41: NO_x emission prediction model using LM algorithm for 700 series buses

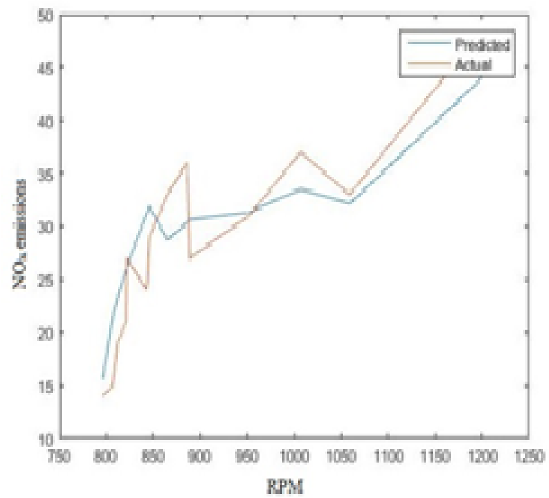

Figure 4-42: NO_x emission prediction model using LM algorithm for 800 series buses

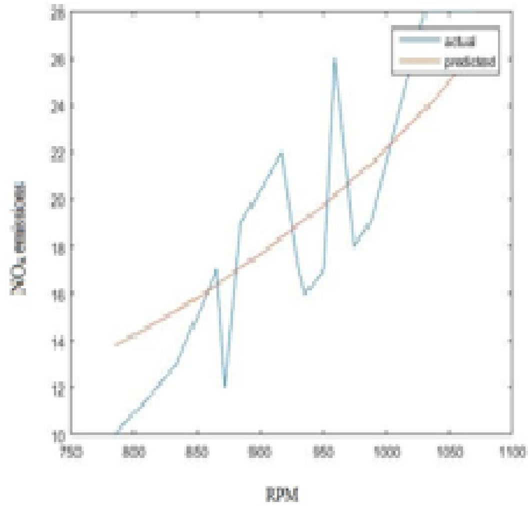

Figure 4-43: NO_x emission prediction model using SVMR algorithm for 700 series buses

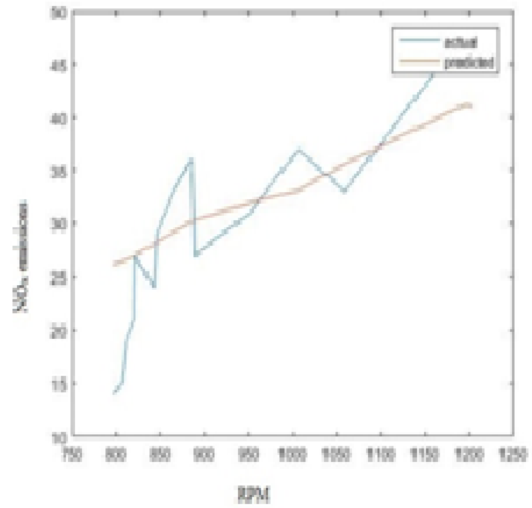

Figure 4-44: NO_x emission prediction model using SVMR algorithm for 800 series buses

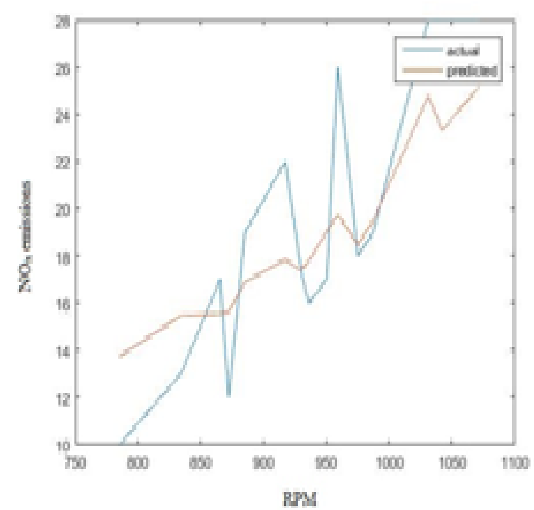

Figure 4-45: NO_x emission prediction model using RFR algorithm for 700 series buses

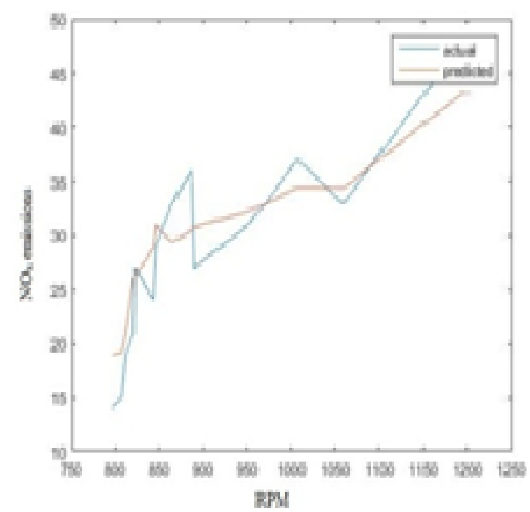

Figure 4-46: NO_x emission prediction model using RFR algorithm for 800 series buses

The best fit for the error coefficients in the deceleration case for the 700 series buses and the 800 series buses are 2.52 and 3.27, respectively, both attained while using the RFR algorithm.The best fit for the error coefficients from the models for the three different techniques while using different number of neurons depending on the dataset are tabulated in Table 4.3.

Table 4.3: NO_x emission prediction errors for all the cases of the bus fleets

Bus/Condition	**LM(ppm)**	**SVMR(ppm)**	**RFR(ppm)**
700/A	5.80	7.20	5.08
800/A	10.47	7.80	6.64
700/MVS	9.20	6.57	4.57
800/MVS	8.78	7.76	7.37
700/D	2.67	2.86	2.52
800/D	3.46	4.95	3.27
700/C	2.29	2.04	1.96
800/C	5.14	2.98	2.55
700/H	1.53	3.21	0.92
800/H	3.87	3.05	0.86

4.3 NO_x emission prediction model

The regression models were employed to study and predict NO_x emission values obtained in all the running conditions of the bus. However, it was difficult to get predictive equations for the software. For the simplification of future studies and to simplify research problems, a set of equations have been developed to predict NO_x emission values for the different running conditions of the buses. The equations were approximated using the curve fitting tool in MATLAB and the set of equations were mostly polynomials and depend on the different parameters considered while running the field experiments.

In the idle conditions of the buses, the parameters needed for the prediction of the NO_x emission values are the idle time (in seconds) denoted by x and the engine coolant temperature for the 700 series buses, and the EGR temperature for the 800 series buses denoted by y. The models for both the EGR and NON-EGR equipped engines in the hot and cold idling cases have been approximated to a set of linear polynomial equations as seen below. The root mean squared error for the created models in the cold idling and hot idling condition for the NON-EGR and EGR engine buses are 2.273, 1.792 ,0.6618 and 0.7939, respectively. The ideal value of mean square error is 1.38. The values of the constants and the generalized model form, represented by f(x,y) for the cold idling and hot idling cases for both sets of buses are presented below.

Cold Idling:

Linear polynomial model for the 700 series buses

$$f(x,y) = 414.3 - 70.22x + 4.508y + 225.4x^2 - 363.6xy + 166.3y^2 + 501x^3 - \\ 1564x^2y + 1586xy^2 - 534.9y^3 + 93.33x^4 - 471.8x^3y + 631.2x^2y^2 - 254.8xy^3 \tag{4.1}$$

Linear polynomial model for the 800 series buses

$$f(x,y) = 279.1 - 81.15x + 16.67y + 107.9x^2 - 153.8xy + 65.95y^2 - 82.77x^3 + \\ 258.1x^2y - 270.4xy^2 + 86.59y^3 - 6.386x^4 - 37.64x^3y + 82.76x^2y^2 - 36.18xy^3 \tag{4.2}$$

Hot Idling:

Linear polynomial model for the 700 series buses

$$f(x,y) = 240.6 - 23.24x + 0.5915y - 11.84x^2 - 16.24xy - 6.609y^2 + 20.419x^3 + \\ 59.39x^2y + 55.41xy^2 + 16.69y^3 - 0.6025x^4 - 9.959x^3y - 13.11x^2y^2 - 4.826xy^3 \tag{4.3}$$

Linear polynomial model for the 800 series buses

$$\begin{aligned} f(x,y) = 193.6 - 29.11x + 0.1058y - 2.128x^2 + 9.662xy - 6.1y^2 + 22.14x^3 - \\ 64.5x^2y + 63.51xy^2 - 20.72y^3 - 33.9x^4 + 100.4x^3y - 98.81x^2y^2 + 32.44xy^3 \end{aligned} \tag{4.4}$$

In the initial running condition of the buses, the parameter needed for the prediction of NO_x emission values is the rpm value of the buses denoted by the variable x in the models, f(x). The model is approximated to a general Gauss model in the acceleration mode and the constants are mentioned below. The root mean squared error for the 700 series and the 800 series buses are 6.708 and 6.866, respectively.

Initial Acceleration:

Linear polynomial model for the 700 series buses

$$f(x) = 7.831x^5 - 3.386x^4 - 40.63x^3 + 8.612x^2 + 110.8x + 530.4$$

Gauss model for the 800 series buses

$$\begin{aligned} f(x) = 265.3e^{-(\frac{x-1.887}{0.8547})^2} + 346.2e^{-(\frac{x-0.3149}{2.081})^2} + 23.56_3^{-(\frac{x+0.656}{0.08509})^2} + \\ 18.02e^{-(\frac{x+0.2759}{0.1875})^2} + 195.6e^{-(\frac{x+1.753}{1.129})^2} \end{aligned} \tag{4.5}$$

In the motion with variable speed mode, the NO_x emissions for the EGR and NON-EGR engine equipped buses were approximated to a linear polynomial model for the 800 series buses and a general Fourier model for the 700 series buses. The root mean squared error for the polynomial and Fourier model are 7.016 and 7.592 respectively.

Variable Speed Mode:

General Fourier model for the 700 series buses

$$f(x) = -225.8 + 19.5\cos(xw) + 115.2\sin(xw) - 16.07\cos(2xw) - 39.26\sin(2xw) + \\ 17.25\cos(3xw) - 5.649\sin(3xw) - 12.33\cos(4xw) - 7.956\sin(4xw) + \\ 7.282\cos(5xw) - 1.146\sin(5xw) + 0.4768\cos(6xw) + 1.575\sin(6xw) \tag{4.6}$$

Linear polynomial model for the 800 series buses

$$f(x) = 3.619x^4 + 11.57x^3 - 1.27x^2 + 8.649x + 158.7$$

In the deceleration mode of the buses, the parameter needed for the prediction of NO_x emission values is the rpm value of the buses. The model is approximated to a linear polynomial model in the deceleration mode and the root mean squared errors in the NON-EGR and EGR engine buses are 2.468 and 2.902 respectively.

Deceleration Mode:

Linear polynomial model for the 700 series buses

$$f(x) = 0.7257x^2 + 4.787x - 19.39$$

Linear polynomial model for the 800 series buses

$$f(x) = -1.613x^6 + 6.764x^5 - 6.711x^4 - 2.146x^3 + 4.457x^2 + 3.551x + 31.71$$

In the partial idling mode, the time period for which the buses come to a halt is taken as a parameter required for the prediction of NO_x emission values. The models for both NON-EGR and EGR equipped engine buses was approximated to a general Fourier model and the root mean squared errors are 6.492 and 1.631 respectively.

Partial Idling:

General Fourier model for the 700 series buses

$$f(x) = 160.8 + 133\cos(1.041x) + 80.93\sin(1.041x) - 12.11\cos(2.082x) - 50.91(2.082x)$$

General Fourier model for the 800 series buses

$$f(x) = 177.7 + 63.59\cos(1.46x) + 19.23\sin(1.46x) - 7.597\cos(2.92x) - 51.16\sin(2.92x) - 8.051\cos(4.38x) + 17.4\sin(4.38x) + 5.619\cos(5.84x) - 13.12\sin(5.84x) - 10.25\cos(7.3x) + 3.803\sin(7.3x) + 2.054\cos(8.76x) + 3.387\sin(8.76x) \tag{4.7}$$

4.4 Elemental analysis of Particulate Matter Samples

In order to characterize the elemental composition of the soot samples an elemental analysis using ICP-MS and EDS/SEM was conducted. By using ICP-MS, a bulk analysis of the soot samples was obtained whereas EDS/SEM was useful in obtaining a surface analysis. Furthermore, ICP-MS results gave the information pertaining to trace metals concentrations (Na, Mg, Al, P, K, Ca, Fe, Cu, and Mo) which were present in the soot samples. On the other hand, EDS/SEM was used to obtain measurements of C, O, Si, and Cu concentrations. Thus, each analysis technique was used to measure the concentrations of elements which were expected to be present in the sample, and together a complete picture could be formed. Tables 4.4, 4.5, 4.6, and 4.7.

The tables show the concentrations of 8 major elements present: Na, Mg, Al, P, K, Ca, Fe, Cu, and Mo. Based on previous studies [53, 54], the source of these elements was most likely from the fuel although other sources could possibly be fuel additives, lubricants, and wears from engine parts (piston rings, bearings, bushings, etc.). The

Table 4.4: ICP-MS results of composition of blank quartz filter paper

	Blank Paper			
Elements	**1**	**2**	**3**	**Avg (μg/g)**
Na	96.70	109.30	96.45	100.82
Mg	96.95	97.50	100.15	98.20
Al	45.11	45.28	45.56	45.32
P	18.00	15.49	15.74	16.41
K	18.92	19.96	18.37	19.08
Ca	ND	ND	ND	ND
Fe	10.96	10.91	11.92	11.27
Cu	5.84	5.73	5.72	5.76
Mo	ND	ND	ND	ND

concentration values for the 700 and 800 series samples were adjusted by subtracting the concentrations of the blank sample. These values are labeled as adjusted. ND indicates no detection which means that the element was at a concentration below the limit of detection (LOD). The threshold concentrations for LOD are found in Table 4.7.

As shown in Tables 4.4 and 4.5, the concentrations of the elements in the 700 series were generally higher than the 800 series. Previous studies have shown that elements such as sodium can serve as precursors for PM formation. Thus, the higher concentration of these elements suggests that there was a larger amount of PM emissions in the 700 series. Because of the 700 series lacked EGR equipped engines, the higher concentration of PM was expected.

Phosphorous, potassium, and Iron were detected in the each sample. The presence of these elements in each sample indicates the temperature and EGR equipment did not make a significant change in the emission of these elements. A potential source for iron could be from the rusting of engine parts whereas potassium and phosphorous

Table 4.5: ICP-MS results of the PM samples:(700 series)

	700 Cold					700 Hot				
Elements	1	2	3	Avg (μg/g)	Adjusted	1	2	3	Avg (μg/g)	Adjusted
Na	204.73	204.08	204.93	204.58	103.76	176.64	175.74	175.09	175.82	100.81
g	135.01	141.53	144.92	140.49	42.28	93.61	95.21	95.26	94.69	98.20
Al	355.88	355.38	353.59	354.95	309.63	171.54	170.79	171.24	171.19	45.31
P	55.58	59.01	61.55	58.72	42.30	74.84	71.24	72.39	72.82	16.40
K	41.76	40.82	41.62	41.40	22.31	38.95	38.42	37.91	38.43	19.08
Ca	252.79	233.86	142.28	209.64	209.64	ND	ND	ND	ND	ND
Fe	34.52	34.83	34.85	34.73	23.46	29.04	29.13	28.89	29.02	11.26
Cu	3.83	3.89	3.74	3.82	ND	3.40	3.48	3.49	3.46	5.76
Mo	ND	ND	ND	ND	ND	ND	ND	ND	ND	ND

Table 4.6: ICP-MS results of the PM samples: (800 series)

	800 Cold					800 Hot				
Elements	1	2	3	Avg (μg/g)	Adjusted	1	2	3	Avg (μg/g)	Adjusted
Na	77.04	77.24	76.94	77.09	ND	118.05	118.30	118.36	118.25	17.43
g	75.44	76.54	76.14	76.04	ND	92.48	92.18	92.58	92.38	ND
Al	33.63	33.66	41.95	36.41	ND	60.18	60.13	59.93	60.08	14.76
P	43.79	42.51	44.95	43.75	27.33	67.50	70.91	65.70	68.05	51.64
K	30.10	29.25	29.24	29.53	10.44	36.85	35.26	35.24	35.78	16.70
Ca	178.59	267.63	177.69	208.00	208.00	265.80	314.44	204.26	261.48	261.48
Fe	21.67	22.38	22.56	22.20	10.93	52.91	53.26	53.31	53.16	41.89
Cu	3.05	3.73	4.27	3.68	ND	6.07	6.14	6.06	6.09	0.32
Mo	1.35	1.44	1.41	1.40	1.40	1.72	1.70	1.67	1.70	1.69

Table 4.7: Limit of detection for the ICP-MS analysis

Elements	**LOD (μg/g)**
Na	0.75
Mg	0.72
Al	0.46
P	135.96
K	0.93
Ca	135.56
Fe	0.33
Cu	0.03
Mo	0.10

most likely came from the fuel or lubricants.

Sodium and aluminum were detected in 700 cold, 700 hot and 800 hot samples. The concentrations of sodium and aluminum were particularly high in the 700 series samples due to the absence of exhaust gas recirculation. Aluminum was the most abundant element in the 700 cold sample with an average composition of 41.1%. The elevated levels of aluminum is most likely from engine wear. Sodium was the most abundant element in the 700 hot series sample with an average composition of 33.9%. Higher temperatures are thought to be the reason for the elevated concentrations of sodium. These higher temperatures could also explain the presence of sodium in the 800 hot series sample.

Calcium was detected in the 700 cold, 800 cold, and 800 hot samples. Furthermore, calcium was by far the most abundant element in the 800 series sample with an average composition of 80.5% and 64.4% for the cold and hot samples, respectively. Calcium was reported as a typical marker for exhaust emissions due to its presence in both fuel and lubricating oil. Therefore, calcium's presence in the soot samples was expected.

Table 4.8: ICP-MS results showing percent composition

Elements	**700 Cold % elements**	**700 Hot % elements**	**800 Cold % elements**	**800 Hot % elements**
Na	13.7	33.9	ND	4.2
Mg	5.6	33.1	ND	ND
Al	41.1	15.2	ND	3.6
P	5.6	5.5	10.58	12.7
K	2.9	6.4	4.10	4.1
Ca	27.8	ND	80.5	64.4
Fe	3.2	5.7	4.20	10.3
Cu	ND	1.9	ND	0.07
Mo	ND	ND	0.54	0.41

Also, the high concentrations of calcium in the 800 series samples indicate that the extra exhaust filtration may do little to reduce calcium emissions. Lastly, copper was detected in the 700 hot and 800 hot samples, and Molybdenum detected in the 800 cold and 800 hot samples.

In order to assess the validity of our results we compared our results with previous studies. [55] compared diesel emissions to emissions from biodiesel. Inductively coupled plasma optical emission spectrometry (ICP-OES) was used to measure the concentration of trace metals. It was found that the concentrations of calcium, magnesium, and iron were in higher concentration in biodiesel than in diesel [55]. The higher concentration of magnesium was in good agreement with our measurements for the 700 series samples. However, the 800 series samples did not detect any magnesium. This may be due to the increased extra filtering with the 800 series. Furthermore, the higher concentration of calcium was in good agreement with our measurements at each condition except for at 700 hot. Iron was also present in each of our samples. The origin of these metals was considered to be from the biodiesel fuel itself and not from engine wear due to biodiesels self-lubricating properties [55].

EDS/SEM results: An EDS/SEM analysis was used to give a surface analysis of the samples. EDS analysis was also useful in giving measurements of carbon and oxygen concentrations which could not be found using ICP-MS. Figs. 4.47 - 4.51 show the SEM results of this analysis.

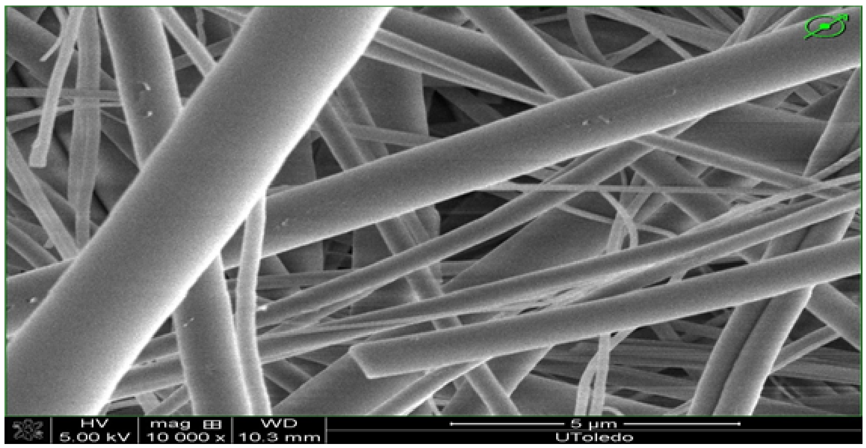

Figure 4-47: Image of blank filter paper showing membrane fibers without deposits

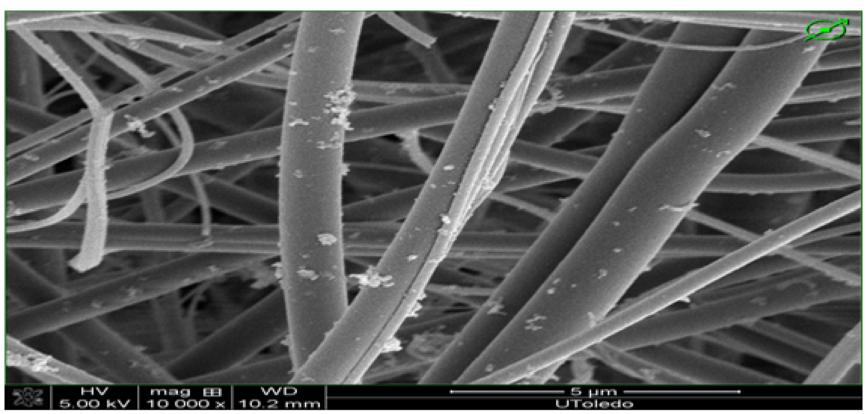

Figure 4-48: SEM image of 700 Cold idling sample filter paper showing membrane fibers with deposits

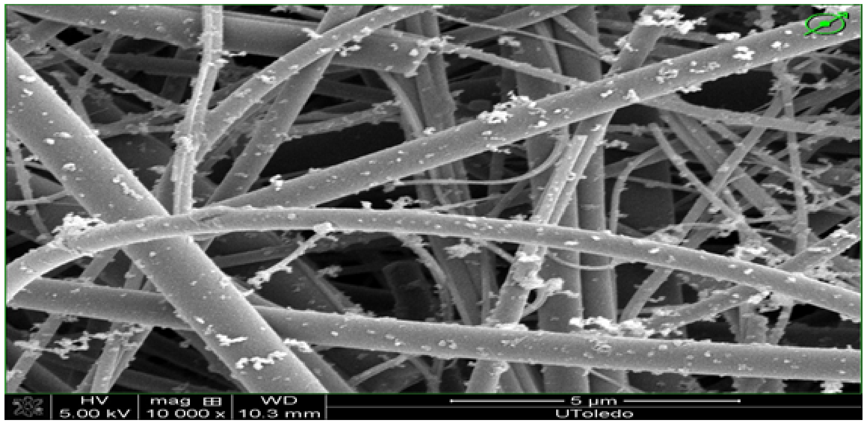

Figure 4-49: SEM image of 700 hot idling sample filter paper showing membrane fibers with deposits

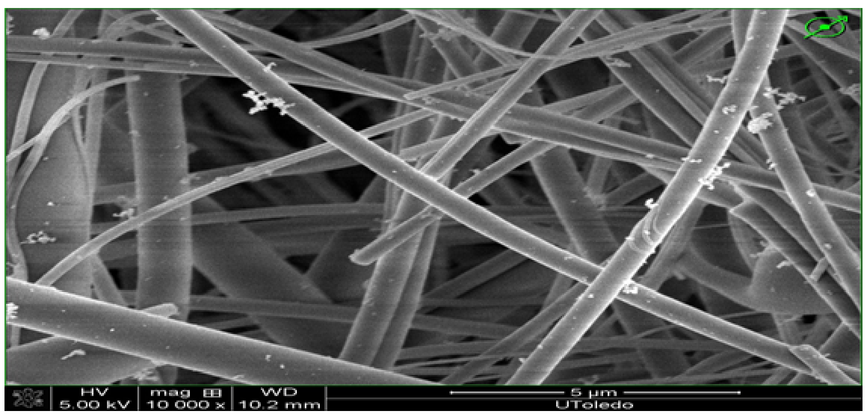

Figure 4-50: SEM image of 800 Cold idling sample filter paper showing membrane fibers with deposits

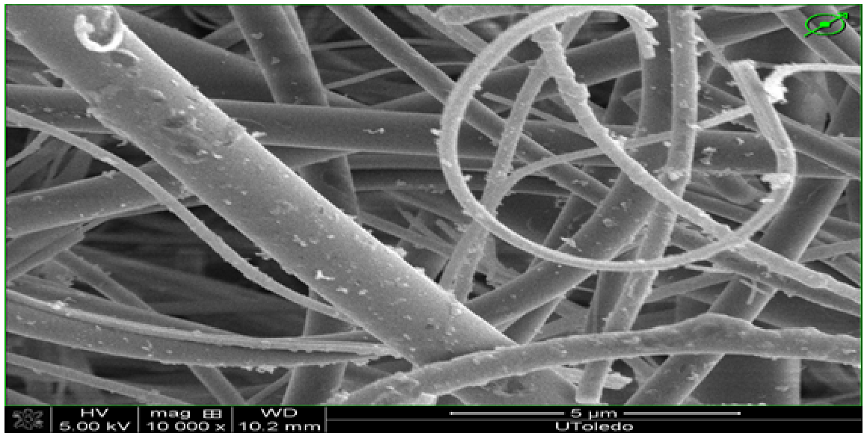

Figure 4-51: SEM image of 800 hot idling sample filter paper showing membrane fibers with deposits

The presence of soot is clearly shown in the 700 and 800 series images which is indicated by the deposits on the strands of a filter membrane. The blank sample image only shows the strands of a filter membrane without any deposits. The 700 series samples seems to show a larger amount of deposits on the membrane fibers when compared to the 800 series, which was expected because of the lack of EGR equipped engine on the 700 series. Also, the hot samples for both the 700 and 800 series seem to a show a larger around of PM. Based on previous studies, a larger amount of soot was expected for the hot temperature condition because of the increased formation of methane at higher temperatures which is a precursor for soot formation. However, it should be mentioned that drawing conclusions about the concentrations of soot from the images could lead to erroneous conclusions because only a small section of the sample could be analyzed at a time.

The EDS results were then used to draw a more quantitative comparison of the concentrations of C, O, Si, and Cu. The Table 4.9 summarizes the EDS results:

Table 4.9: EDS results of different elements for all cases of PM samples

Element	**Blank** (%)	**700 Cold** (%)	**700 Hot** (%)	**800 Cold** (%)	**800 Hot** (%)
C	8.81	15.25	20.48	8.8	11.29
O	65.08	64.77	60.79	67.5	63.06
Si	25.52	19.56	18.34	23.29	25.11
Cu	0.59	0.41	0.38	0.40	0.53

Carbon was found to be in higher concentrations in the 700 series samples. The higher carbon contents in the 700 series could be attributed to the lack of filtering from the exhaust pipes of the 700 series buses. Furthermore, the higher carbon contents could indicate the presence of a larger amount of PM as soot has been shown to be mostly composed of carbon. In the 800 series the exhaust pipes undergo an extra set of filtering which could remove soot. Also, there seems to be an increase in the carbon content between cold and hot idling. As mentioned previously, increased methane formation is expected at elevated temperatures which could be a possible explanation for the higher carbon content in the hot idling samples. When comparing the oxygen, silicon and copper content between the blank sample and soot samples, it was found that the O, Si, and Cu presence in the soot samples was negligible.

[55] studied the amount of elemental carbon present at various engine conditions. For this analysis, a total organic carbon (TOC) analyzer was used. It was found that the amount of elemental carbon was highest at the idling engine condition and decreased as engine load increased [55]. Our EDS/SEM results agreed with the presence elemental carbon during both cold and hot idling, with a larger amount present

at the hot idling condition. We were not able to confirm the effect of engine load as both samples were taken during idling conditions.

Chapter 5

Conclusion

Successful field experiments were carried out to study the tail pipe emissions from transit buses in real day to day life. Tail Pipe emission studies in this thesis concentrated on NO_x and PM emissions which were carried out on different types of TARTA buses and were evaluated under different conditions. To exhibit the effect of the various type of engines, EGR and NON-EGR equipped engine buses were used as part of the experiments while considering various engine parameters. The research was broadly divided into two sections: (a) study of NO_x emission data and, (b) study of particulate matter emitted from the exhaust of the respective buses.

The NO_x emissions study was carried out in two phases-collection and analysis. The collection phase was split into idle and running conditions. Data was collected and categorized under various cases such as cold and hot idling, acceleration and deceleration, variable speed mode and partial idling. Horiba NO_x analyzer was used to collect data in all these cases. Regression techniques and the curve fitting tool were used to analyze the data collected. Prediction models and equations were developed from this analysis. The PM emissions study was carried out by collecting the PM data using a catch can instrument and quartz filter papers. Energy dispersive spectroscopy (EDS) and inductively coupled plasma mass spectroscopy (ICP-MS) was performed on the particulate matter data collected.

A comprehensive field testing protocol which included the addition of regression techniques was developed for better evaluation and analysis of NO_x emissions from TARTA buses. A few major findings from the study have been explained below.

1. It was observed from the tail-pipe emission values obtained from both EGR and Non-EGR equipped engine buses that the 700 series buses have higher NO_x emissions when compared to the 800 series buses. This result was in direct correlation to the fact that the 700 series buses do not possess EGR exhausts and hence no filtering is done before the emissions are let out into the atmosphere. Emission values considered in all the different conditions and modes of the buses also prove that there was a significant difference of 30-35% between the 700 series and the 800 series buses.

2. Hotter engines produce lesser emissions when compared to colder engine conditions. This performance was found to be consistent among both fleets of buses.

3. From the NO_x emission values obtained from both fleets of buses, it was inferred that maximum emissions were found in the initial acceleration condition followed by cold idling, variable speed mode, hot idling, and the least values were obtained from the deceleration condition. Partial idling condition values were not examined for analysis as data collected was unreliable due to the short time intervals and was considered to get a general description of the NO_x emissions.

4. Equation models were developed for all the conditions of the buses using the Curve fitting tool of MATLAB. Many factors were involved in estimating the NO_x emissions during the running condition of the bus such as varied road and climatic conditions, passenger load, air conditioned load, speed,etc. Of

all the various factors, the speed (rpm) of the bus was seen to be a major constraint while collecting the NO_x emission values and was considered as the independent variable for the curve fitting. In the cold and hot idling conditions, five different parameters were considered as independent variables in order to obtain a relation with the NO_x emissions values (in ppm).

5. In the running condition of the buses, NO_x emission values were known to be directly dependent on the speed (rpm) of the buses. The NO_x emission values increased as the speed of the buses increased and vice-versa.

6. The NO_x emission values recorded in the idling mode were found to be mainly dependent on engine temperature, exhaust gas pressure, fuel flow rate command, diesel oxidation catalyst intake temperature and the diesel particulate filter intake temperature. In the idling mode, an increase in time lead to an increase in engine temperature thereby reducing the NO_x emission values. The values recorded in this stage were not dependent on speed due to the stationary position of the buses.

7. Regression techniques were used to analyze the NO_x emission data collected and then to predict NO_x emission values. Three different methods were employed. The RFR algorithm proved to be the best method to predict emission values as it provided with the least error in all the conditions of the experiments. The SVM method and the LM method also provided us small errors but were not as efficient as the RFR algorithm.

8. It was also perceived that the behavior of pollutants was not constant with the age of the vehicle but higher failures were noted in older buses. Proper maintenance and the replacement of old buses with new ones equipped with EGR engines proved to reduce NO_x emissions by about 25-35% as seen.

PM data was collected with the help of a catch can instrument and quartz filter papers. The EDS and ICP-MS analysis gave us quite a few valuable inferences. They are summarized below.

1. Concentrations of the following trace metals: Na, Mg, Al, P, K, Ca, Fe, Cu, and Mo were found to be in generally higher concentration in the 700 series than the 800 series. This higher concentration was expected because of the lack of EGR equipment with the 700 series.

2. A surface analysis via SEM imaging showed a larger amount of soot deposits for the 700 series samples which was expected because of the lack of EGR equipment. Furthermore, the sample at a hot temperature condition showed a larger amount of PM formation. The larger amount of PM formation at elevated temperatures could be attributed to increased methane formation at higher temperatures which is a precursor for soot formation.

3. Carbon was found to be at a higher concentration in the 700 series when compared to the 800 series which could indicate a larger amount of PM formation. There also seems to be an increase in carbon content between cold and hot idling.

5.1 Future Work

In view of the major findings of this study, a few areas of further development and investigation are recommended, mainly:

1. Study of different biodiesel blends such as B40, B50 and more on transit buses having EGR and NON-EGR equipped engines.

2. Detailed study of NO_x emission data in the running condition of the buses also factoring in all the major engine parameters in addition to the speed (rpm).

3. Advanced techniques for PM matter collection during the running conditions of the bus.

4. Study of PM and NO_x emissions during different operation modes may lead to better identification and understanding of the variables involved.

References

[1] C. Ris, "US EPA health assessment for diesel engine exhaust: a review," *Inhalation Toxicology*, vol. 19, no. sup1, pp. 229–239, 2007.

[2] J. Pinsker, "Yes, Rush Hour Traffic is getting worse," 2015. [Online]. Available: http://www.theatlantic.com/business/archive/2015/08/rush-hour-traffic-commute/402418/

[3] "Wardsauto," 2015. [Online]. Available: http://wardsauto.com/news-analysis/world-vehicle-population-tops-1-billion-units

[4] "American Public Transportation Association (APTA)." [Online]. Available: http://www.apta.com/mediacenter/pressreleases/2015/pages/150309_ridership.aspx

[5] M. Dickens and J. Neff, "APTA 2014 Public Transportation Fact Book," 2014. [Online]. Available: https://www.apta.com/resources/statistics/Documents/FactBook/2014-APTA-Fact-Book.pdf

[6] G. Knothe, C. A. Sharp, and T. W. Ryan, "Exhaust emissions of biodiesel, petrodiesel, neat methyl esters, and alkanes in a new technology engine," *Energy & Fuels*, vol. 20, no. 1, pp. 403–408, 2006.

[7] W. H. Organization, *Air quality guidelines: global update 2005: particulate matter, ozone, nitrogen dioxide, and sulfur dioxide.* World Health Organization, 2006.

[8] M. Redel-Macías, S. Pinzi, M. Ruz, A. Cubero-Atienza, and M. Dorado, "Biodiesel from saturated and monounsaturated fatty acid methyl esters and their influence over noise and air pollution," *Fuel*, vol. 97, pp. 751–756, 2012.

[9] N. Nylund, K. Erkkilä, M. Lappi, and M. Ikonen, "Transit bus emission study: comparison of emissions from diesel and natural gas buses," in *IANGVA Conference, Buenos Aires, Argentina*, 2004.

[10] K. A. Baumert, T. Herzog, and J. Pershing, *Navigating the numbers: Greenhouse gas data and international climate policy.* World Resources Inst, 2005.

[11] "U.S EPA, Mobile Source Emissions-Past, Present and Future," 2015. [Online]. Available: http://www.epa.gov/otaq/invntory/overview/pollutants/nox.html

[12] "U.S Environmental Protection Agency," 2016. [Online]. Available: https://www.epa.gov/newsreleases/epa-report-diesel-engine-grants-program-nets-major-air-public-health-benefits-0

[13] Environmental Protection Agency, "A Comprehensive Analysis of Biodiesel Impacts on Exhaust Emissions," 2002.

[14] N. Künzli, R. Kaiser, S. Medina, M. Studnicka, O. Chanel, P. Filliger, M. Herry, F. Horak, V. Puybonnieux-Texier, P. Quénel *et al.*, "Public-health impact of outdoor and traffic-related air pollution: a european assessment," *The Lancet*, vol. 356, no. 9232, pp. 795–801, 2000.

[15] M. Lapuerta, O. Armas, and J. Rodriguez-Fernandez, "Effect of biodiesel fuels on diesel engine emissions," *Progress in energy and combustion science*, vol. 34, no. 2, pp. 198–223, 2008.

[16] C. Gierczak, G. Jesion, J. Piatak, and J. Butler, "On-board vehicle emissions

measurement program: Crc ve-11-1," *Coordinating Research Council, Washington, D.C*, 1994.

[17] N. A. Kelly and P. J. Groblicki, "Real-world emissions from a modern production vehicle driven in los angeles," *Air & Waste*, vol. 43, no. 10, pp. 1351–1357, 1993.

[18] M. J. St. Denis, P. Cicero-Fernández, A. M. Winer, J. W. Butler, and G. Jesion, "Effects of in-use driving conditions and vehicle/engine operating parameters on âĂIJoff-cycleâĂİ events: Comparison with federal test procedure conditions," *Air & Waste*, vol. 44, no. 1, pp. 31–38, 1994.

[19] S. Bari, "Performance, combustion and emission tests of a metro-bus running on biodiesel-ulsd blended (b20) fuel," *Applied Energy*, vol. 124, pp. 35–43, 2014.

[20] A. Sydbom, A. Blomberg, S. Parnia, N. Stenfors, T. Sandström, and S. Dahlen, "Health effects of diesel exhaust emissions," *European Respiratory Journal*, vol. 17, no. 4, pp. 733–746, 2001.

[21] P. Cicero-Fernández, J. R. Long, and A. M. Winer, "Effects of grades and other loads on on-road emissions of hydrocarbons and carbon monoxide," *Journal of the Air & Waste Management Association*, vol. 47, no. 8, pp. 898–904, 1997.

[22] D. C. Somuri, "Study of particulate number concentrations in buses running with bio diesel and ultra low sulfur diesel," 2011.

[23] J. K. Mwangi, W.-J. Lee, J.-H. Tsai, T. S. Wu *et al.*, "Emission reductions of nitrogen oxides, particulate matter and polycyclic aromatic hydrocarbons by using microalgae biodiesel, butanol and water in diesel engine," *Aerosol Air Qual. Res*, vol. 15, pp. 901–914, 2015.

[24] M. Ergeneman, C. Sorusbay, and A. Goktan, "Exhaust emission and fuel con-

sumption of cng diesel fueled city buses calculated using a sample driving cycle," *Energy sources*, vol. 21, no. 3, pp. 257–268, 1999.

[25] D. Pawel, R. Leggett, K. Eckerman, and C. Nelson, "Uncertainties in cancer risk coefficients for environmental exposure to radionuclides," *ORNL/TM-2006/583, Oak Ridge National Laboratory, Oak Ridge, TN*, 2007.

[26] J. P. Szybist, S. R. Kirby, and A. L. Boehman, "Nox emissions of alternative diesel fuels: a comparative analysis of biodiesel and ft diesel," *Energy & fuels*, vol. 19, no. 4, pp. 1484–1492, 2005.

[27] J. Yanowitz, R. L. McCormick, and M. S. Graboski, "In-use emissions from heavy-duty diesel vehicles," *Environmental Science & Technology*, vol. 34, no. 5, pp. 729–740, 2000.

[28] M. E. Tat, P. S. Wang, J. H. Van Gerpen, and T. E. Clemente, "Exhaust emissions from an engine fueled with biodiesel from high-oleic soybeans," *Journal of the American Oil Chemists' Society*, vol. 84, no. 9, pp. 865–869, 2007.

[29] B. S. Chauhan, N. Kumar, and H. M. Cho, "A study on the performance and emission of a diesel engine fueled with jatropha biodiesel oil and its blends," *Energy*, vol. 37, no. 1, pp. 616–622, 2012.

[30] C. Rakopoulos, D. Rakopoulos, D. Hountalas, E. Giakoumis, and E. Andritsakis, "Performance and emissions of bus engine using blends of diesel fuel with biodiesel of sunflower or cottonseed oils derived from greek feedstock," *Fuel*, vol. 87, no. 2, pp. 147–157, 2008.

[31] M. Delucchi, "Emissions of criteria pollutants, toxic air pollutants, and greenhouse gases, from the use of alternative transportation modes and fuels," *University of California Transportation Center*, 1996.

[32] J. A. Calcagno, "Evaluation of heavy-duty diesel vehicle emissions during cold-start and steady-state idling conditions and reduction of emissions from a truck-stop electrification program," *PhD Diss, University of Tennessee*, 2005.

[33] A. Vijayan, A. Kumar, and M. Abraham, "Experimental analysis of vehicle operation parameters affecting emission behavior of public transport buses with alternative diesel fuels," *Transportation Research Record: Journal of the Transportation Research Board*, no. 2058, pp. 68–78, 2008.

[34] G. A. Ban-Weiss, J. Chen, B. A. Buchholz, and R. W. Dibble, "A numerical investigation into the anomalous slight no x increase when burning biodiesel; a new (old) theory," *Fuel processing technology*, vol. 88, no. 7, pp. 659–667, 2007.

[35] S. K. Hoekman and C. Robbins, "Review of the effects of biodiesel on nox emissions," *Fuel Processing Technology*, vol. 96, pp. 237–249, 2012.

[36] H. C. Frey, A. Unal, N. M. Rouphail, and J. D. Colyar, "On-road measurement of vehicle tailpipe emissions using a portable instrument," *Journal of the Air & Waste Management Association*, vol. 53, no. 8, pp. 992–1002, 2003.

[37] R. L. McCormick, M. S. Graboski, T. L. Alleman, and J. Yanowitz, "Idle emissions from heavy-duty diesel and natural gas vehicles at high altitude," *Journal of the Air & Waste Management Association*, vol. 50, no. 11, pp. 1992–1998, 2000.

[38] K. Shandilya and A. Kumar, "Carbon specification of exhaust particulate matter of public transit buses running on alternative fuels," *Fuel*, vol. 115, pp. 678–684, 2014.

[39] C. E. Wilson, "Biodiesel promise," *Bulk Transporter*, vol. 68, no. 5, 2005.

[40] T. Su, C. Chang, R. D. Reitz, P. Farrell, A. Pierpont, and T. Tow, "Effects of injection pressure and nozzle geometry on spray smd and di emissions," SAE Technical Paper, Tech. Rep., 1995.

[41] "Toledo area regional transit authority, mechanics handbook," 2015.

[42] H. Gavin, "The Levenberg-Marquardt method for nonlinear least squares curve-fitting problems," 2011.

[43] B. M. Wilamowski, S. Iplikci, O. Kaynak, and M. Ö. Efe, "An algorithm for fast convergence in training neural networks," in *International Joint Conference on Neural Networks*, vol. 3, 2001, pp. 1778–1782.

[44] L. Breiman, "Random forests," *Machine learning*, vol. 45, no. 1, pp. 5–32, 2001.

[45] S. Adusumilli, D. Bhatt, H. Wang, P. Bhattacharya, and V. Devabhaktuni, "A low-cost ins/gps integration methodology based on random forest regression," *Expert Systems with Applications*, vol. 40, no. 11, pp. 4653–4659, 2013.

[46] V. Svetnik, A. Liaw, C. Tong, J. C. Culberson, R. P. Sheridan, and B. P. Feuston, "Random forest: a classification and regression tool for compound classification and qsar modeling," *Journal of chemical information and computer sciences*, vol. 43, no. 6, pp. 1947–1958, 2003.

[47] D. R. Cutler, T. C. Edwards, K. H. Beard, A. Cutler, K. T. Hess, J. Gibson, and J. J. Lawler, "Random forests for classification in ecology," *Ecology*, vol. 88, no. 11, pp. 2783–2792, 2007.

[48] R. Díaz-Uriarte and S. A. De Andres, "Gene selection and classification of microarray data using random forest," *BMC bioinformatics*, vol. 7, no. 1, p. 1, 2006.

[49] B. Larivière and D. Van den Poel, "Predicting customer retention and profitability by using random forests and regression forests techniques," *Expert Systems with Applications*, vol. 29, no. 2, pp. 472–484, 2005.

[50] J. A. Suykens and J. Vandewalle, "Training multilayer perceptron classifiers based on a modified support vector method," *IEEE Transactions on Neural Networks*, vol. 10, no. 4, pp. 907–911, 1999.

[51] B. Schölkopf, A. J. Smola, R. C. Williamson, and P. L. Bartlett, "New support vector algorithms," *Neural computation*, vol. 12, no. 5, pp. 1207–1245, 2000.

[52] D. Bhatt, P. Aggarwal, V. Devabhaktuni, and P. Bhattacharya, "A novel hybrid fusion algorithm to bridge the period of gps outages using low-cost ins," *Expert Systems with Applications*, vol. 41, no. 5, pp. 2166–2173, 2014.

[53] H. Omidvarborna, A. Kumar, and D. S. Kim, "Characterization of particulate matter emitted from transit buses fueled with b20 in idle modes," *Journal of Environmental Chemical Engineering*, vol. 2, no. 4, pp. 2335–2342, 2014.

[54] K. Shandilya and A. Kumar, "Particulate emissions from tailpipe during idling of public transit buses fueled with alternative fuels," *Environmental Progress & Sustainable Energy*, vol. 32, no. 4, pp. 1134–1142, 2013.

[55] A. K. Agarwal, T. Gupta, and A. Kothari, "Particulate emissions from biodiesel vs diesel fuelled compression ignition engine," *Renewable and Sustainable Energy Reviews*, vol. 15, no. 6, pp. 3278–3300, 2011.